24

The Configuration of Jupiter's Magnetosphere

Krishan K. Khurana, Margaret G. Kivelson
Institute for Geophysics and Planetary Physics, University of California, Los Angeles

Vytenis M. Vasyliunas, Norbert Krupp, Joachim Woch, Andreas Lagg
Max-Planck-Institut für Aeronomie, Katlenburg-Lindau

Barry H. Mauk
The Johns Hopkins University Applied Physics Laboratory

William S. Kurth
Department of Physics and Astronomy, University of Iowa

24.1 INTRODUCTION

A magnetosphere is a "sphere" of influence around a planet in which the forces associated with the magnetic field of the planet prevail over all other forces. The magnetic field of the planet diverts the solar wind away from the planet, carving a cavity which contains a low-density hot plasma derived from the solar wind, or the planet. The plasmas of the solar wind and the magnetosphere are kept apart by a thin boundary layer called magnetopause in which strong surface currents circulate. To form and maintain a magnetosphere, three key ingredients are required. These are, a strong enough planetary magnetic field that halts the solar wind, a source of plasma internal or external to the magnetosphere to populate it and a source of energy to power it. The solar wind driven magnetospheres (of which the Earth and Mercury are prime examples) derive their plasma and energy mainly from the solar wind. In rotationally driven magnetospheres, the bulk of the energy is derived from planet's rotation whereas the plasma is derived from the planet or a satellite of the planet (jovian and kronian magnetospheres are the prime examples of this category).

The interior of Jupiter is the seat of a strong dynamo that produces a surface magnetic field in the equatorial region with an intensity of ~ 4 Gauss. This strong magnetic field and Jupiter's fast rotation (rotation period $\sim$ 9 h 55 min) create a unique magnetosphere in the solar system which is known for its immense size (average subsolar magnetopause distance 45-100 R_J where 1 R_J = 71492 km is the radius of Jupiter) and fast rotation (see Figure 24.1 for a schematic of Jupiter's magnetosphere). Jupiter's magnetosphere differs from most other magnetospheres in the fact that it derives much of its plasma internally from Jupiter's moon Io. The heavy plasma, consisting principally of various charge states of S and O, inflates the magnetosphere from the combined actions of centrifugal force and thermal pressure. It is readily shown that in the absence of an internal heavy plasma, the dipole field would balance the average dy-

namic pressure of the solar wind (0.08 nPa) at a distance of ~ 42 R_J in the subsolar region as contrasted to the observed average magnetopause location of $\sim$75 R_J (see Figure 24.1). The heavy plasma is also responsible for generating an azimuthal current exceeding 160 MA in the equatorial region of Jupiter's magnetosphere where it is confined to a thin current sheet (half thickness ~ 2 R_J in the dawn sector).

It is traditional to divide Jupiter's magnetosphere into inner ($<$10 R_J), middle (10-40 R_J) and outer ($>$40R_J) regions. The inner magnetosphere is the seat of plasma production for the magnetosphere and it also hosts the inner radiation belts. It is estimated that Io's plasma torus located between the radial distances of ~ 5.2 and ~ 10 R_J contains several million tons of plasma which slowly diffuses outward aided by instabilities feeding on the centrifugal force. Because of the strong internal magnetic field and the low temperature of the torus plasma (E $<$ 100 eV for the core of the ion distribution), the plasma β (ratio of particle energy density to magnetic energy density) is $<$ 0.2 in most of this region and the effects of plasma on the magnetic field are minimal. However, the effect of magnetic field on the distribution and energetics of the plasma is profound. As any charged particle experiences a strong Lorentz force ($= q\mathbf{V} \times \mathbf{B}$)when moving across the field, the spatial distributions of the particles tend to be strongly organized by the field direction, being much more homogeneous along the field than across it. A description of the internal field, therefore, greatly aids in understanding the plasma source populations and the ionosphere-magnetosphere coupling. Unfortunately, only the lowest harmonics (less than fourth order) of the jovian field can be determined accurately because of the limited radial and azimuthal range coverage of the Jupiter bound spacecraft. In the inner magnetosphere, the warm and cold plasma of the torus is confined to the centrifugal equator, a surface defined by the loci of points where each field line reaches its farthest distance from the rotational axis of Jupiter.
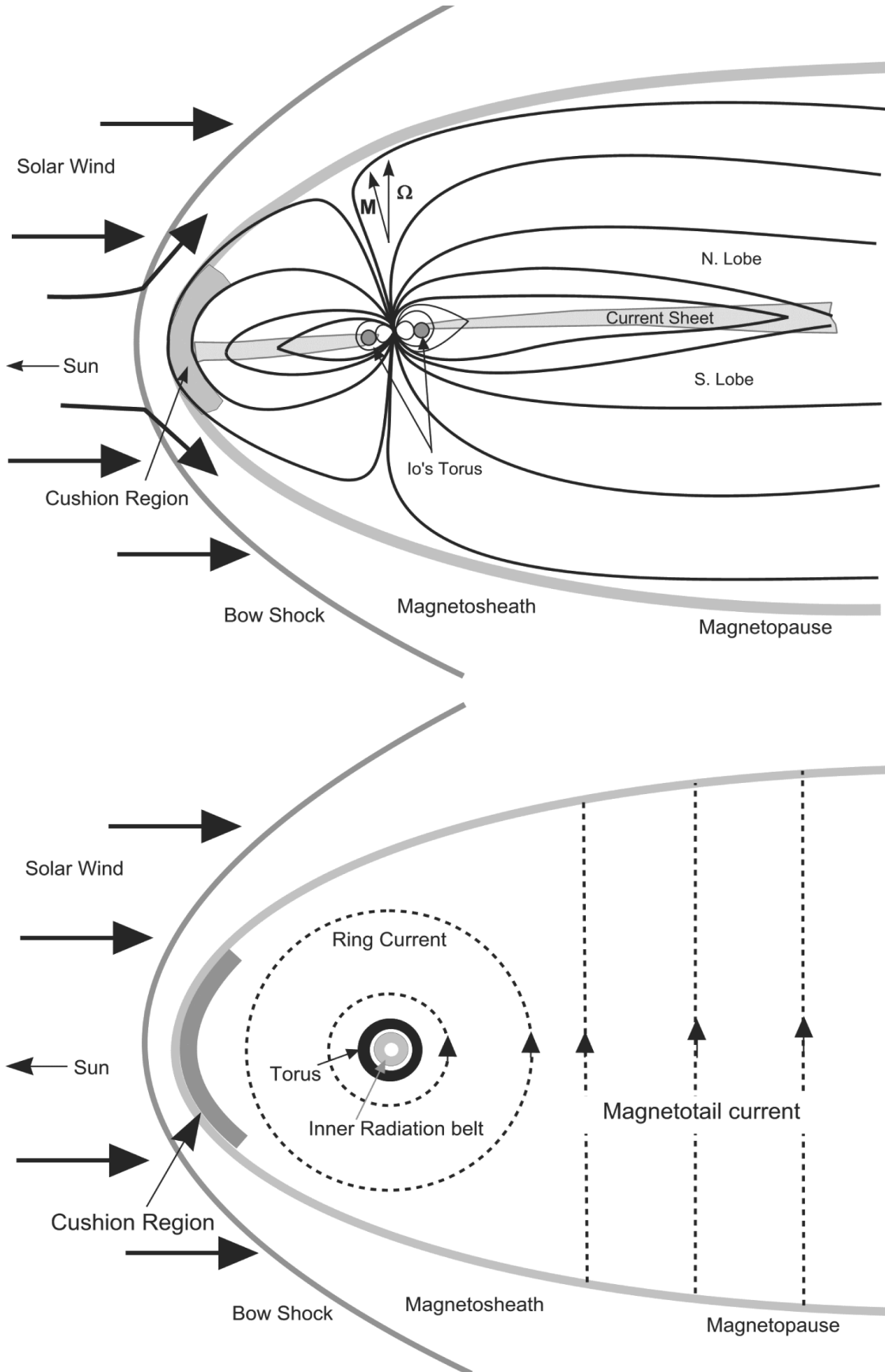
Figure 24.1. A schematic of Jupiter's magnetosphere showing the noon-midnight meridian (top) and the equatorial cross-section (bottom).

In the middle magnetosphere, the plasma corotation with Jupiter's magnetosphere gradually breaks down because the poorly conducting ionosphere of Jupiter is not able to impart sufficient angular momentum to the outflowing plasma. The radial currents, which enforce corotation on the magnetospheric plasma, generate aurorae in the jovian ionosphere by accelerating electrons into the ionosphere from the action of large field-aligned potentials. In the thin current sheet located near the equatorial plane of Jupiter, the azimuthal currents are very large and create magnetic field perturbations which are comparable in magnitude to the internal field beyond a radial distance of ~ 20 R$_J$. The plasma β also exceeds unity in the current sheet beyond this distance. In this region the magnetic field becomes highly stretched as it acts to contain the plasma against the strong centrifugal and thermal pressure forces. The current sheet assumes a complex structure because the solar wind dynamic pressure, the particle thermal pressure and the centrifugal force are equally important in determining its location. In addition, the current sheet becomes systematically delayed from the magnetic dipole equator because in a noncorotating plasma, the information on the location of the dipole has to be continually propagated outwards from the inner magnetosphere. The plasma temperature is quite high ($T_i > 10$ keV) and it is not fully understood what process or processes are responsible for energizing the warm plasmato such high values in this region. New observations from *Galileo* show that the field and current strengths are not axially symmetric in Jupiter's magnetosphere but show local time asymmetries similar to those observed in the Earth's magnetosphere. This finding suggests that the solar wind quite likely drives a convection system in Jupiter's magnetosphere in ways analogous to the Earth's magnetosphere.

In the outer magnetosphere, the azimuthal plasma velocity lags corotation by a factor of two or more. The outer magnetosphere on the dayside is extremely squishy. Depending on the solar wind dynamic pressure, the dayside magnetopause can be found anywhere from a distance of ~ 45 R$_J$ to 100 R$_J$ (Joy *et al.* 2002). An extremely disturbed region with a radial extent of ~ 15 R$_J$ was discovered adjacent to the noon magnetopause in the magnetic field observations from *Pioneer* and *Voyager* spacecraft. Because, the magnetic field is oriented strongly southward, this disturbed region must be located inside the magnetosphere but the familiar ten-hour periodicity in the magnetic field is absent. It is not yet known whether this region known as "the cushion region" is a permanent or a temporal feature of the magnetosphere. Finally, in the nightside outer magnetosphere, an additional current system exists that connects the magnetodisc current to the magnetopause currents. This current system, called the magnetotail current system further stretches the magnetic field lines, creating a long magnetotail (length > 7000 R$_J$), which has been known to extend to the orbit of Saturn. The magnetospheric regions above and below the current sheet are depleted of plasma ($n_e < 0.01$ /cm^3) and currents ($J < 0.01$ nA/m^2) and are referred to as lobes (see Figure 24.1) in analogy with similar regions found in the Earth's magnetotail.

Excluding *Cassini*, which mainly skimmed the dusk boundary region in December 2000, six spacecraft have explored the magnetosphere of Jupiter. *Pioneer 10* flew by Jupiter in December of 1973 on a low inclination trajec-
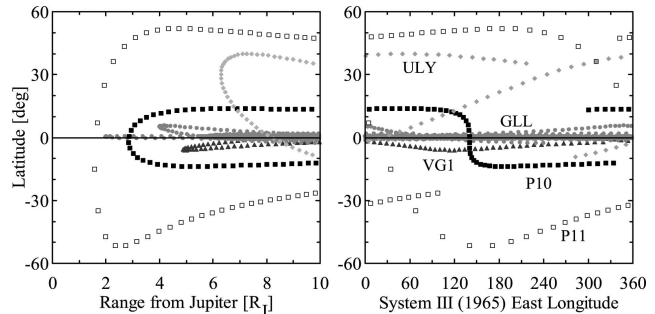

Figure 24.2. Trajectories of all spacecraft that have visited Jupiter at a distance of < 10 R$_J$.

tory (S III latitude $< 15°$) that brought it within 2.8 R$_J$ from Jupiter's center. *Pioneer 10* confirmed the presence of a strong magnetic field in Jupiter and showed that Jupiter's magnetosphere is extremely large. *Pioneer* 11 arrived at Jupiter in the December of 1974 on a highly inclined trajectory (maximum S III latitude 52°) that brought it within 1.6 R$_J$ of Jupiter's center. Because of its retrograde orbit and its high inclination, *Pioneer 11* has provided the best description of the internal field so far. *Voyager 1* and 2 visited Jupiter in March and July of 1979 on nearly equatorial trajectories, with closest approach distances of 4.9 R$_J$ and 10.1 R$_J$, respectively. *Voyager 1* discovered a dense plasma torus of heavy ions near Io's orbit whereas *Voyager* 2 revealed the equatorial current sheet of Jupiter in an unprecedented detail. *Ulysses* flew by Jupiter in the February of 1992 on a mid-latitude trajectory with the closest approach distance of 6.3 R$_J$ from Jupiter's center. *Ulysses* was the first spacecraft to explore the dusk high latitude region of Jupiter. Finally, *Galileo* has been orbiting Jupiter since December 1995. After exploring the magnetotail of Jupiter in the prime mission, the spacecraft has now completed its investigations of the dusk and post-noon sectors of Jupiter's magnetosphere. Thus, the six spacecraft between them have completely mapped the low-latitude regions of the magnetosphere over all local times.

In the next section, we begin our survey of Jupiter's magnetosphere starting from the inner magnetosphere. This chapter deals with the concepts relating to the configuration and structure of the magnetosphere and the processes involved in a steady state equilibrium of the magnetosphere. The temporal dynamics of the magnetosphere resulting from the loading and unloading of plasmas from Io's plasma torus and the solar wind are covered in Chapter 25 (Krupp *et al.*). The inner magnetosphere is covered in further detail from the viewpoint of cold plasma population in Chapter 23 (Thomas *et al.*) and energetic plasma populations in Chapter 27 (Bolton *et al.*). The magnetospheric processes that power the jovian aurorae are covered in considerable detail in Chapter 26 (Clarke *et al.*).

24.2   THE INNER MAGNETOSPHERE

24.2.1   Internal Magnetic Field

A knowledge of the magnetic field of a magnetosphere aids in the understanding of (1) the particle dynamics (bounce and drift of plasma in the magnetosphere, plasma diffusion

into and out of the radiation belts, changes in the pitch angle distributions of plasma from convection etc.); (2) the magnetospheric dynamics (magnetic storms and substorms, interchange instabilities, generation and propagation of MHD waves etc.); and (3) phenomena and processes that couple the magnetosphere to the ionosphere (convection electric fields imposed upon the ionosphere, origin of auroral precipitating particles etc.). Unfortunately, a direct sampling of the magnetic field has been possible only over a limited radial and latitudinal range of Jupiter. The measurements from a single spacecraft also cannot distinguish between the spatial and temporal changes observed along the spacecraft trajectory. Magnetic field models which satisfy Maxwell's equations and certain stress balance requirements are therefore constructed to predict the average field in regions where no data exist.

The magnetic field observed at a location can be represented as the sum of an internal field, $\mathbf{B}_i$ arising from currents internal to the planet, and an external field, $\mathbf{B}_e$, arising from current sources present in the magnetosphere and the ionosphere. Thus

$$\mathbf{B} = \mathbf{B}_i + \mathbf{B}_e \tag{1}$$

The external field arises from current systems that exist in the jovian current sheet, the magnetopause and field lines that couple Jupiter's ionosphere to its magnetosphere. These are discussed in the sections on middle and outer magnetospheres.

The internal magnetic field can be represented as the gradient of a scalar potential such that $\mathbf{B}_i = -\nabla\Phi_i$. The scalar potential satisfies the Laplace equation $\nabla^2\mathbf{B} = 0$ whose solution in a spherical coordinate system (r, θ, λ) is given by the sum of spherical harmonics:

$$\Phi_i = \sum_{l=1}^{\infty} \left(\frac{R}{r}\right)^{l+1} \sum_{m=0}^{l} P_l^m(\cos\theta) \tag{2}$$
$$[g_l^m \cos(m\lambda) + h_l^m \sin(m\lambda)]$$

where R is the planet's radius, r is the distance from the center of the planet, θ and λ are the colatitude (measured from the planet's spin pole) and the longitude of the observer, P_l^m are the associated Legendre polynomial functions (see Arfken (1985) for their definition), and g_l^m, h_l^m are the Schmidt coefficients of order l and degree m determined from the observations. If observations are available everywhere on a closed surface surrounding the volume space in which the magnetic field is being generated, equation (2) can be inverted with extreme precision. However, the observations are most commonly available along a single or multiple orbits of the planet. In such a case only certain coefficients can be obtained accurately. In general, for a dynamo field, the amplitudes of the Schmidt coefficients decrease with increasing order (l number). Therefore, higher order terms are more difficult to resolve from a limited data set.

Figure 24.2 shows the trajectories (inside a radial distance of 10 R_J) of all of the spacecraft that have visited Jupiter including the final orbits of *Galileo* before its demise in an impact with Jupiter in September 2003. Whereas the retrograde flyby of *Pioneer 11* provided excellent coverage of the mid to high latitude regions, *Pioneer 10* provided good measurements of the equatorial current sheet. Data

from these two spacecraft provided the basis for the first two models, JPL P11 (Davis *et al.* 1975) and O_4 (Acuna and Ness, 1976) which included the first three orders and degrees of the spherical harmonics. Connerney (1992) later included observations from the *Voyager 1* flyby to derive an 18 eigenvalue solution called the O_6 model by fitting the data to a sixth order spherical harmonic expansion. (However, coefficients for only the first three orders are reliable.) Connerney also included the contribution of the jovian current sheet to the observed magnetic field in his fit. Dougherty *et al.* (1996) assessed the O_6 model against magnetic field measurements made by *Ulysses* and concluded that overall the O6 model provides an excellent match to the observations but suggested that better fits would be obtained if the axial dipole term (g_1^0) were reduced by 0.189 G from 4.242 G to 4.053 G.

Connerney (1992) has shown that in situ observations are not yet good enough to constrain terms higher than the third order. A recent model (VIP4) put forward by Connerney *et al.* (1998) uses both the in situ spacecraft data (*Pioneer* and *Voyager*) and information on the location of the Io footprint in Jupiter's ionosphere. The VIP4 model includes terms up to $l = 4$ and was constructed so that the observed footprints of Io would map to a radial distance of 5.9 R_J, the radial distance of Io.

Another model optimized for the inner magnetosphere is by Randall (1998) who showed that none of the existing models can reproduce the absorption microsignature of the jovian satellite Amalthea observed by *Pioneer 11*. By modifying the *Pioneer* models of internal magnetic field, Randall was able to derive a new model that produced a reasonable fit to the microsignature. However, it is not known how well this model is able to predict the location of the Io footprint. Table 24.1 lists the spherical harmonic coefficients of all of the major models which are currently in use. Because of the limited latitudinal coverage, the observations from *Galileo* have not yet been able to improve upon these models.

A good measure of the global field of a planet is the strength and direction of its dipole field. The three first order terms, g_1^0, g_1^1 and h_1^1, can be thought of as the moments of three dipoles oriented along the z, x and y axes of the jovigraphic system of coordinates in which the z axis is aligned along the jovian axis of rotation, x-axis is oriented in the equatorial plane and points along the System III prime meridian and the y-axis completes the triad. (This coordinate system is opposite to System III convention which is left handed and increases with time as described in Appendix 2.) The total dipole magnetic moment $|M|$ (expressed as strength of the surface field at the magnetic equator) is thus given by

$$|M| = \sqrt{(g_1^0)^2 + (g_1^1)^2 + (h_1^1)^2} \tag{3}$$

and the dipole tilt θ_M and its orientation λ_M are given by

$$\theta_M = \tan^{-1}(\sqrt{(g_1^1)^2 + (h_1^1)^2}/g_1^0) \tag{4}$$

$$\lambda_M = \tan^{-1}(h_1^1/g_1^1) \tag{5}$$

The lower part of Table 24.1 lists the dipole parameters for the models discussed above.

Table 24.1. Spherical harmonic coefficients and dipole characteristics of some major models. In this and other descriptions of the magnetic field of Jupiter, the right handed System III coordinates are used for which the longitude increases in the eastern direction (decreases with time).

Term/Parameter	P11 [1]	O4 [2]	O6 [3]	*Ulysses* [4]	VIP4 [5]	Amalthea [6]
g_1^0	4.144	4.218	4.242	4.053	4.205	4.132
g_1^1	-0.692	-0.664	-0.659	-0.692	-0.659	-0.692
h_1^1	0.235	0.264	0.241	0.235	0.250	0.216
g_2^0	0.036	-0.203	-0.022	0.036	-0.051	0.041
g_2^1	-0.581	-0.735	-0.711	-0.581	-0.619	-0.607
h_2^1	0.442	-0.469	0.487	0.442	0.497	-0.416
g_2^2	-0.427	0.513	-0.403	-0.427	-0.361	0.482
h_2^2	0.134	0.088	0.072	0.134	0.053	0.100
g_3^0	-0.047	-0.233	0.075	-0.047	-0.016	0.066
g_3^1	-0.502	-0.076	-0.155	-0.502	-0.520	-0.351
h_3^1	-0.342	-0.588	0.198	-0.342	0.244	-0.292
g_3^2	0.352	0.168	-0.180	0.352	-0.176	0.200
h_3^2	0.296	0.487	-0.388	0.296	-0.088	0.293
g_3^3	-0.136	-0.231	0.342	-0.136	0.408	-0.120
h_3^3	-0.041	-0.294	-0.224	-0.041	-0.316	-0.202
g_4^0					-0.168	
g_4^1					0.222	
h_4^1					-0.061	
g_4^2					-0.202	
h_4^2					$\sim$	
g_4^3					$\sim$	
h_4^3					0.404	
g_4^4					-0.166	
h_4^4					$\sim$	
M (Gauss)	4.208	4.278	4.300	4.118	4.264	4.195
θ_M(deg)	10.0	9.6	9.4	10.2	9.5	10.0
λ_M(deg) RH	161.2	158.3	159.9	161.2	159.2	162.7

[1] *Pioneer 11* model is from Davis *et al.* 1975. [2] O4 model is from Acuna and Ness (1976). [3] O6 model is reproduced from Connerney (1992). [4] *Ulysses* model is described in Dougherty *et al.* (1996). [5] VIP4 model is reproduced from Connerney *et al.* (1998). [6] Amalthea model is from Randall (1998).

Since Jupiter does not have a solid surface, the rotation period of its interior has traditionally been gauged from its magnetic field. Two different techniques have been used for this purpose. In one technique, the radio waves at decametric or decimetric wavelengths from plasma populations trapped in Jupiter's magnetic field measured either at Earth or in space have been used to define the System III rotation period (Hide and Stannard, 1976). The radio waves at decametric wavelengths are emitted from several sources, some fixed in System III longitude. Therefore, by following the rotation of these sources over long periods, one can determine the rotation period of Jupiter. The decimetric waves are beamed in a small cone around the instantaneous velocity vector of the relativistic electrons. Because, the plasma is confined mainly to the tilted rotating magnetic equator, the beaming geometry between the observer and the radiating population has a diurnal period. The beaming curve or the polarization of decimetric waves if observed continuously over a long period can be used to define the rotation period of Jupiter.

The second technique makes use of the in situ measurements of the magnetic field. The azimuthal orientation (λ_M) of the dipole vector obtained from a spherical analysis of in situ data from different epochs can be used to define the rotation period and look for secular variations in the magnetic field. Using this technique, Connerney and

Acuna (1982) concluded that System III provided an excellent measure of the rotation period of Jupiter and that no detectable changes in Jupiter's internal field had occurred over the period covered by *Pioneer* and *Voyager* spacecraft. Recently, Russell *et al.* (2001) have applied this technique to the *Galileo* data and concluded that the azimuthal orientation of the dipole has changed by less than 0.01°/yr. This drift is much smaller than the value proposed by Higgins *et al.* (1997) from radio observations ($\sim 0.25°$/yr).

24.2.2 The Inner Magnetosphere: The Plasma Sources

In situ and remote observations of Io and its surroundings from *Voyager* showed that Io is the main source of plasma in Jupiter's magnetosphere (Bagenal and Sullivan, 1981, Broadfoot *et al.* 1981, Hill *et al.* 1983). It is estimated that upward of 6×10^{29} amu/s (~ 1 ton/s) of plasma mass is added to the magnetosphere by Io. The picked-up plasma consists mostly of various charged states of S and O and populates a torus region extending from a radial distance of 5.2 R_J to ~ 10 R_J. Bagenal and Sullivan (1981), Bagenal *et al.* (1985) and Scudder et al., (1981) provided the first measurements of the density, temperature and structure of Io's torus. The torus was found to be divided into an inner cold region ($T_i \approx 2$-10 eV) where ions are tightly confined

to the centrifugal equator and an outer warm torus region ($T_i \approx 60$ eV) where the scale height of ions is ~ 1 R$_J$. It is understood that the high density and the cold temperature of the inner torus reflects the long residence time of ions in the cold torus where they are subject to significant cooling. In the warm torus, the iogenic plasma diffuses outward under the stress of centrifugal force while the more energetic plasma from Jupiter's plasma sheet diffuses inward (Siscoe *et al.* 1981). We refer the reader to chapter 25 (Thomas *et al.* 2003) for a detailed look at the properties of plasma torus.

The next most important source of plasma in Jupiter's magnetosphere is the solar wind whose source strength can be estimated by a consideration of the solar wind mass flux incident on Jupiter's magnetopause and the fractional amount that makes it into the magnetosphere ($< 1\%$). Such a calculation suggests that the solar wind source strength is < 100 kg/s (Hill *et al.* 1983) considerably lower than the Io source. Nevertheless, the number density of protons (as opposed to the mass density) may be comparable to the iogenic plasma number density in the middle and outer magnetospheres where the solar wind may be able to gain access to the magnetosphere.

The escape of ions (mainly H^+ and H_2^+) from the ionosphere of Jupiter provides the next significant source of plasma in Jupiter's magnetosphere. The ionospheric plasma escapes along field lines when the gravity of Jupiter is not able to contain the hot plasma (~ 10 eV and above). The escape however is not uniform and depends on the local photoelectron density, the temperature variations of the ionosphere with the solar zenith angle, other factors such as the auroral precipitation of ions and electrons and the ionospheric heating from Pedersen currents. In situ measurements show that in Io's torus, protons contribute to less than 20% of total ion number density and constitute $< 1\%$ of mass suggesting that the ionosphere is not a major source of plasma in Jupiter's magnetosphere. Hill *et al.* place the ionospheric source strength to be in the range of ~ 20 kg/s.

Finally, the surface sputtering of the three icy satellites by jovian plasma provides the last significant source of plasma in Jupiter's magnetosphere. Because the icy moons lack extended atmospheres and the fluxes of the incident plasma are low at the locations of these moons, the total pickup of plasma from these satellites is estimated to be less than 20 kg/s based on the plasma sputtering rates provided by Cooper *et al.* (2001).

Other minor constituents found in the torus (Bagenal and Sullivan, 1981) were Na^+ (with an abundance of $< 5\%$) and molecular ions SO^+ and SO_2^+ (both with abundances of $< 1\%$ of the total). The average mass of a torus ion is ~ 20 and the average fractional charge on an ion is ~ 1.2 (McNutt *et al.* 1981). The bulk velocity of the plasma was found to be ~ 75 km/s, close to the corotational value.

24.2.3   The Inner Magnetosphere: The Radiation Belts

The energization of plasma by various electrical fields as it diffuses inwards is responsible for the creation of radiation belts in the inner magnetosphere of Jupiter. It is believed that the radial diffusion is driven by the ionospheric dynamo fields produced by winds in Jupiter's atmosphere (Brice and McDonough, 1973, Schardt and Goertz, 1983).
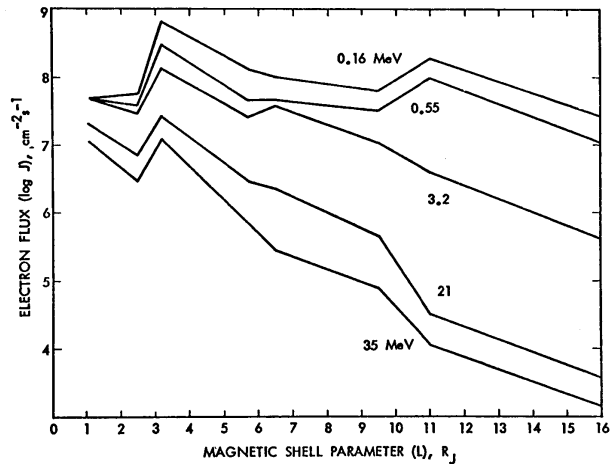

Figure 24.3. Electron fluxes in the inner magnetosphere as modeled by Divine and Garrett (1983). Figure reproduced from Schardt and Goertz (1983).

Figure 24.3 shows the distribution of electrons in the inner magnetosphere calculated from the Divine and Garrett (1983) model based on the *Pioneer* observations. The electrons would be strongly absorbed by Europa (L = 9.5 R$_J$) and Io (L = 5.9 R$_J$) resulting in micro-signatures downstream of these moons. However, the overall impact of such absorption is small and no broad macro-signatures are observed near the orbits of these moons. However, a broad minimum in the electron fluxes is seen to occur near L = 2.5 R$_J$, the L shell of Amalthea. Inside of this distance, further losses occur from interaction of electrons with other minor satellites and the rings of Jupiter. Energetic electron measurements from the *Galileo* Jupiter probe (Mihalov *et al.* 2000) are in broad agreement with the *Pioneer 10* observations. The probe observations show that the energy spectra become softer (especially for smaller pitch angles) as Jupiter is approached (inside of 2 R$_J$), presumably because of energetic electrons' stronger interaction with Jupiter's atmosphere. Recently, Bolton *et al.* (2001) have inverted the observed synchrotron emission from relativistic electrons to derive the spatial and pitch angle distribution of electrons in the radiation belt. They show that the Divine-Garrett model significantly underestimates (by as much as a factor of 5-10) the number density of relativistic electrons and its pitch-angle distribution is also not consistent with the synchrotron emission images.

Figure 24.4 from Trainor *et al.* (1974) shows the profile of proton fluxes observed along the trajectory of *Pioneer 10*. The protons exhibit a peak just outside of Io's orbit. The strong depletion near Io's orbit is caused both by direct absorption by Io and also from charge exchange in Io's plasma torus. Although, *Pioneer* ion fluxes were interpreted as resulting mainly from protons, observations from *Voyager 1* showed that O and S also contribute significantly to the observed fluxes (Vogt *et al.* 1979).

Inside of 3 R$_J$, the energetic relativistic electrons lose energy from synchrotron radiation. The synchrotron radiation is mostly emitted in the decimetric radio band and was first discovered from Earth-based observations by Sloanaker (1959). The imaging and interpretation of this radiation is
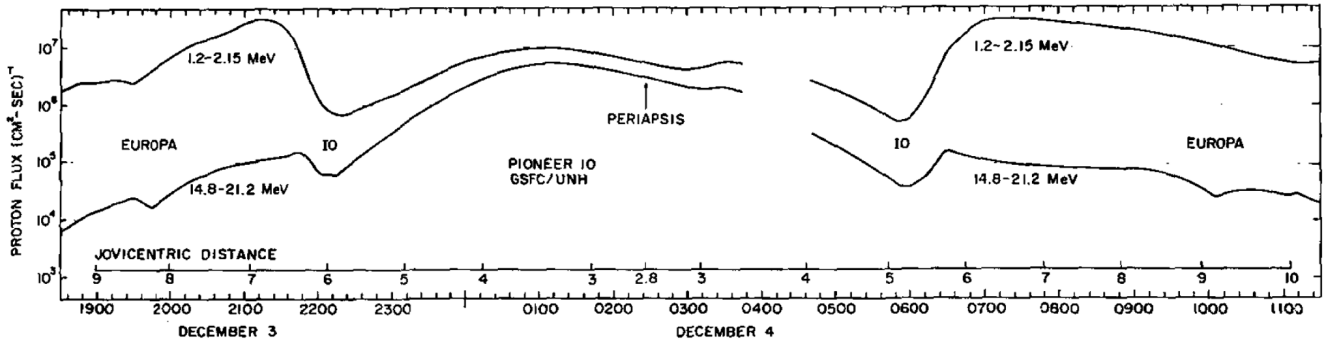
Figure 24.4. Omnidirectional energetic ion fluxes (plotted vs. time in hours) measured by the HET detector along the trajectory of *Pioneer 10*. Figure reproduced from Schardt and Goertz (1983) who adapted it from Trainor *et al.* (1974).
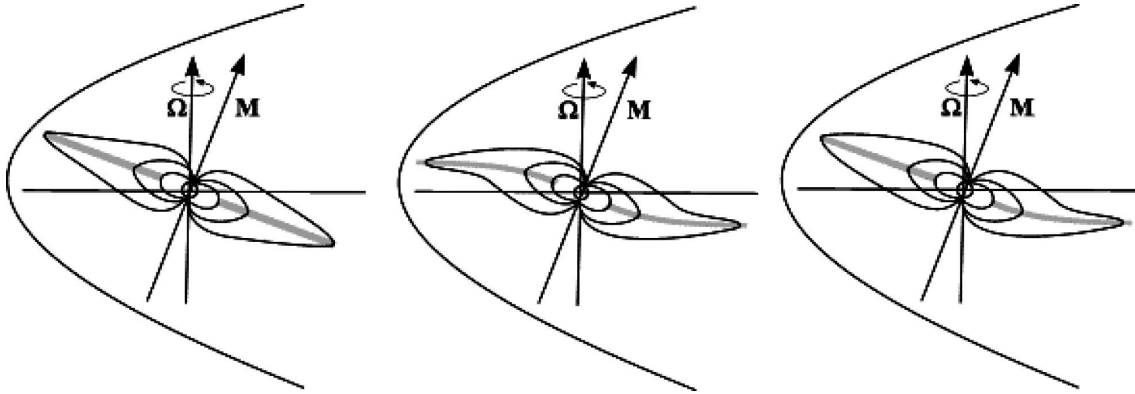

Figure 24.5. The schematics of current sheet structure in the prime meridian (S III $\lambda = 338°$). Shown are, a rigid disc collocated with the dipole magnetic equator (Left), a current sheet hinged by the inertial stresses of the plasma on both day and night sides (center) and a current sheet hinged by the solar wind forcing on the night side (right).

a well-developed field in jovian plasma physics and has provided insights on plasma diffusion, internal magnetic field of Jupiter and the effect of Amalthea on spatial and pitch angle distributions of plasmas. Chapter 27 by Bolton *et al.* in this book provides further details on the inner radiation belts and the synchrotron radiation from Jupiter.

24.3   THE MIDDLE MAGNETOSPHERE

24.3.1   Current Sheet Morphology and Structural Models

Jupiter's vast reservoir of plasma is confined to a thin plasma sheet located close to (but not always at) the dipole magnetic equator. The reason for confinement of plasma to regions where the magnetic field is the weakest lies in the mirror force $(-\mu\nabla_{\parallel}B)$ that every gyrating particle with a magnetic moment $\mu = \frac{1}{2}mv_{\perp}^2/B$ experiences in a non-uniform field. Because plasmas and currents are found more or less in the same sheet-like region, the terms current sheet and plasma sheet, are often used interchangeably to describe this plasma reservoir. In magnetohydrodynamic terms, the location of the current sheet results from a stress balance between the inertial (mainly centrifugal force), thermal and Lorentz forces. The changing field and plasma environment in the magnetosphere ensures that the current sheet is neither planar nor constant in its thickness.

Jupiter's current sheet originates near the orbit of Io, where the magnetic field acts to contain the densely populated inner Io plasma torus against the centrifugal force experienced by the corotating plasma. As the ion and electron temperatures in the inner torus are less than 10 eV, the field-aligned magnetic mirror force experienced by the plasma is rather small and the plasma is free to move along the field lines. In this situation, the plasma comes to rest on each field line at the farthest point from the spin axis of Jupiter. Thus, the plasma is confined to a surface called the centrifugal equator, which is defined by the loci of points where each field line has reached its maximum distance from the rotational axis of Jupiter. By definition, at this surface the axially radial component of magnetic field ($= B_\rho$) is zero. Hill *et al.* 1974, and Vasyliunas, 1983 show that the tilt θ_{CS} of the centrifugal equator with respect to Jupiter's rotational equator is given by

$$\tan\theta_{cs} = z/\rho = \frac{-4/3\tan\alpha\cos\phi}{1\mp\sqrt{1+8/9\tan^2\alpha\cos^2\phi}} \tag{6}$$

where $\alpha = 9.6°$ is the dipole tilt and ϕ is the magnetic longitude. Thus, in the prime meridian (where $\cos\phi = 1$), the tilt of the centrifugal equator is approximately $2\alpha/3 = 6.4°$. Observations from plasma experiment (Bagenal and Sullivan, 1981) and magnetic field experiment (Connerney *et al.* 1982) from *Voyager 1* confirmed that the plasma sheet

is indeed collocated with the centrifugal equator in the cold torus.

In situ observations show that the plasma temperature rises rapidly with radial distance in the outer torus and beyond it. In the middle magnetosphere, the field-aligned component of the centrifugal force $(-m_{i,e} \Omega_J^2 \rho \cdot \mathbf{B}/|\mathbf{B}|)$ experienced by plasma particles becomes much smaller than the magnetic mirror force. The plasma, therefore, tends to collect near the magnetic dipole equatorial plane where the magnetic field is the weakest. Actual observations of the jovian current sheet show that beyond ~ 10 R$_J$ and inside of ~ 30 R$_J$, the center of the current sheet is indeed collocated with the dipole magnetic equator (Behannon *et al.* 1981). Beyond 30 R$_J$, where both the centrifugal and the thermal pressure terms contribute to the stress balance, the current sheet is located somewhere between the centrifugal and the magnetic dipole equators.

External stresses such as the solar wind dynamic pressure can also displace the current sheet. It is expected and indeed confirmed from observations that in the magnetotail at large distances (r > 60 R$_J$), the current sheet becomes parallel to the solar wind flow (Khurana, 1992).

In the description presented above, it was assumed that the plasma is corotating with the planet. This condition implies that a rest frame exists in which the field and plasma are both stationary relative to each other and at any location their opposing stresses remain constant. However, observations show that the plasma is subcorotational beyond a radial distance of ~ 20 R$_J$. In this situation, no global stationary frame can be specified and the plasma is continually subjected to time-varying vertical forces (Vasyliunas, 1983) which act to keep the plasma confined to the magnetic field minimum region. This mutual interaction between the field and plasma causes delays in the arrival of the current sheet at a spacecraft. There are two reasons for this delay. The foremost reason for the current sheet delay is the swept-back configuration of the field lines. As discussed below, the azimuthal stresses exerted by the plasma bend the jovian field lines out of their meridians in the westward sense causing a delay in the equatorial points of the field lines and therefore the current sheet. In addition, there is a further delay of the current sheet which arises from the vertical stresses applied by the magnetic field on the subcorotating plasma. The vertical accelerations of the plasma are mediated by Alfvén waves launched from the ionosphere of Jupiter to impose the rocking of the dipole (with an amplitude of 9.6°) on the outer magnetosphere. Because, the wave propagates at a finite velocity, it takes a considerable time for it to propagate from the ionosphere to the equatorial plane in the outer magnetosphere. The results of these delays of the current sheet is that even though an observer located at the jovigraphic equator observes a ten-hour periodicity in both the field and the particle intensities, she would observe a phase delay in the arrival of the current sheet. The current sheet may also not reach its full latitude, i.e. the current sheet becomes hinged.

Using the concept of a wave packet traveling in a rotating magnetosphere in the presence of a radial flow, Northrop *et al.* (1974) and Goertz (1981) showed that the delay ($d\delta$) in the current sheet location (measured in jovian longitude) is given by:
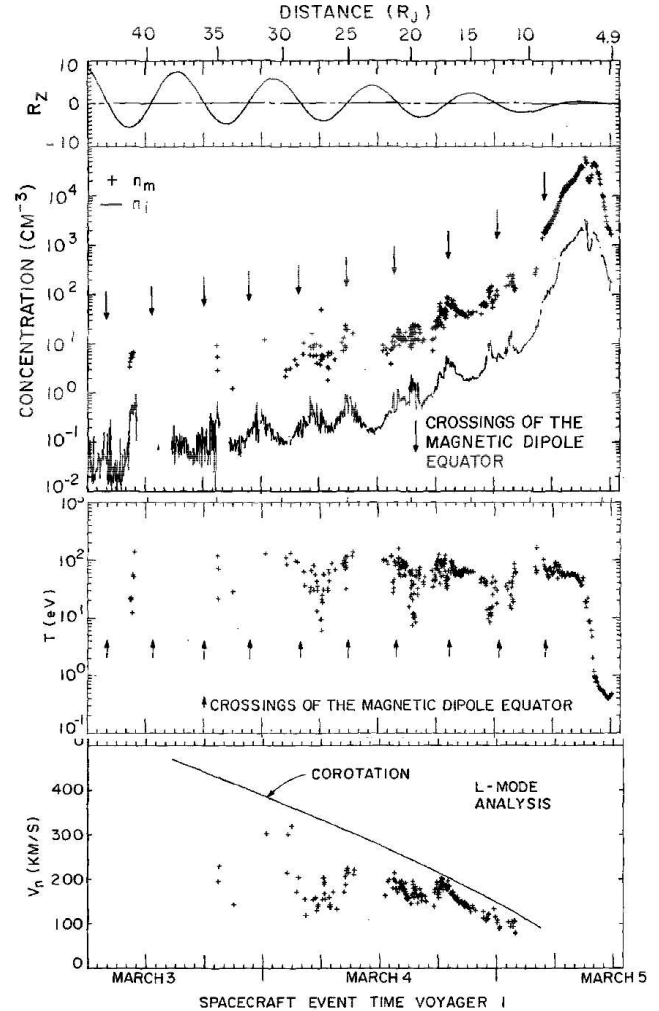

Figure 24.6. The warm plasma parameters in the middle magnetosphere. The top panel shows the distance of the spacecraft from the magnetic dipole equator. The middle panel shows the mass (in amu/cm^3) and charge densities of positive ions. The bottom panel shows the average temperature of the ions which is the sum of the temperatures of the individual species weighted by the number densities. The fourth panel show the component of velocity into the D sensor of the PLS instrument. Also shown is the velocity into the sensor expected for rigid corotation.

$$\frac{d\delta}{d\rho} = \frac{B_\phi}{\rho B_\rho} + \frac{(\Omega_m - \Omega_J)}{(u_\rho + V_A \frac{B_\rho}{B})} \qquad (7)$$

where Ω_J and Ω_m are the angular velocities of Jupiter and its magnetosphere, respectively and V_A is the Alfvén wave velocity. The above equation can be interpreted as follows. The delay results from a combination of two effects, the bend-back of the field line (first term), and the time it takes for the wave to travel through the subcorotating and outflowing ($u_\rho > 0$) plasma in the magnetosphere (the second term on the right hand side).

The field and plasma observations (McKibben and Simpson, 1974; Smith *et al.* 1974; Behannon *et al.* 1981; Schardt *et al.* 1981) indeed show that the current sheet crossings are delayed from the dipole magnetic equator crossings in proportion to the radial distance of the spacecraft from Jupiter. Kivelson *et al.* (1978) modeled the *Pioneer 10* cur-

rent sheets crossings and determined that the wave information propagated outward at a velocity of ~ 43 R$_J$/hr. Further observations from *Voyager* spacecraft showed that when the spacecraft is located above the jovigraphic equator, the north to south crossings are delayed more than the south to north crossings (Behannon *et al.* 1981). These unequal delays can be understood in terms of the hinging of the current sheet (see Figure 24.5, center). A spacecraft located north of the rotational equator would see the hinged current sheet rise to the spacecraft's location (the north to south crossing) slightly later than the nominal time of the current sheet crossing. Similarly, half a rotation later the hinged current sheet would descend to the spacecraft's location, but it would be seen to arrive slightly earlier than its nominal crossing time.

The structural models of Jupiter's current sheet have so far been expressed in System III coordinates. It is typically assumed that the current sheet lies in or near the magnetic dipole equator plane inside of 30 R$_J$, but becomes parallel to the jovigraphic equator (rather than the solar wind flow direction) beyond this distance. Thus, the small tilt between Jupiter's equator and its orbital plane ($3.2°$) is ignored. For example, Behannon *et al.* 1981 expressed the height of the current sheet with respect to Jupiter's equator at a longitude λ as (in a right-handed coordinate system)

$$Z_{cs} = a_0 \tan(9.6°) \tanh\left(\frac{\rho}{a_0}\right) \cos(\lambda - \delta) \qquad (8)$$

where $\delta = \delta_0 - \frac{\Omega_J(\rho - \rho_0)}{U}$ and δ_0 is the longitude of the prime meridian in which the dipole axis is located, a_0 is the hinge point, U is the information propagation speed and ρ_0 is the origin point of wave delay. Behannon *et al.* found that no single common set of fitting parameters (a_0, U, ρ_0) could be found to fit the axially symmetric model of current sheet crossings from *Voyager* and *Pioneer* spacecraft. Khurana, (1992) showed that if one assumed that the current sheet hinging was induced by the solar wind forcing, then a single model of the hinged-magnetodisc can be obtained. He parameterized the hinging distance in terms of Jupiter-Sun-magnetospheric (JSM) x-axis, rewriting (16) as:

$$Z_{cs} = \rho \tan(9.6°)\left[\frac{x_0}{x}\tanh\left(\frac{x}{x_0}\right)\cos(\lambda - \delta)\right] \qquad (9)$$

where $\delta = \delta_0 - \frac{\Omega_J \rho_0}{v_0} \ln \cosh\left(\frac{\rho}{\rho_0}\right)$, δ describes the longitude toward which the current sheet has the maximum tilt, and x_0, ρ_0 and v_0 are the three current sheet structure parameters which describe, respectively, the hinge distance, the radial distance beyond which the wave delay becomes effective and the wave velocity. Thus, in this model the current sheet is initially aligned with the magnetic equator (up to $x = x_0$) and then departs from it toward the jovigraphic equator because of hinging. It is possible that in the middle magnetosphere, the hinging of the current sheet is caused mainly by the inertial stresses as discussed above. Nevertheless, in the outer magnetosphere, the magnetotail must become parallel to the solar wind flow beyond a certain distance.

New observations from *Galileo* in the dawn sector show that the Khurana (1992) model provides fairly robust estimates of the current sheet crossing times. However, in the dusk sector, the observed current sheet crossings occur systematically sooner than the predictions by the Khurana
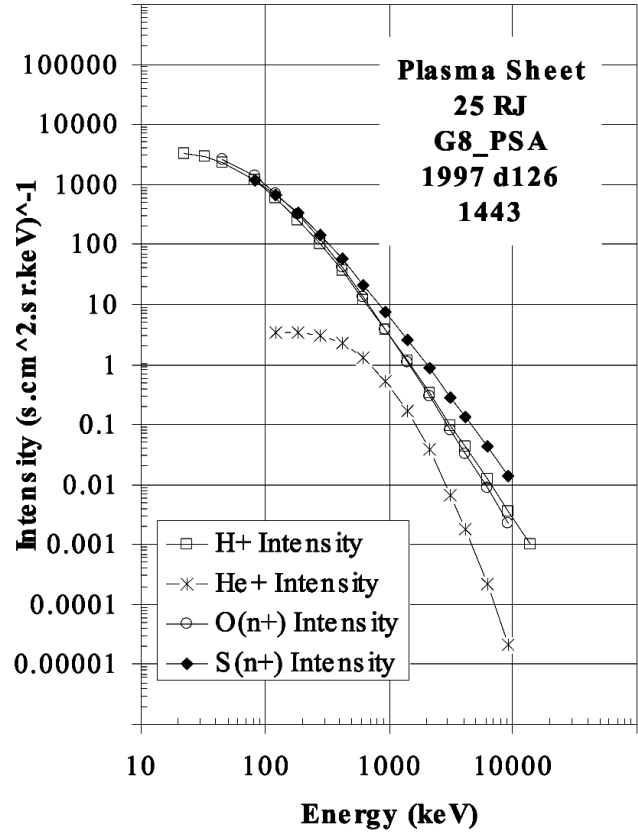

Figure 24.7. Differential fluxes of various charge species at energies > 20 keV measured by the EPD experiment onboard *Galileo* at a radial distance of 25 R$_J$.
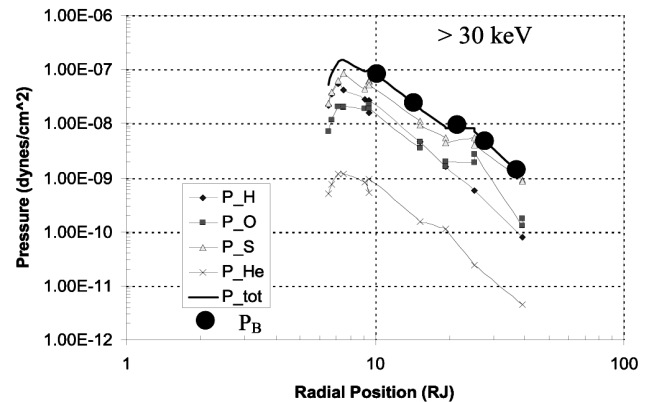

Figure 24.8. The contribution to thermal pressure from various species of the energetic ions in the middle magnetosphere. Shown also in solid filled circles is the magnetic pressure difference between the lobe and the current sheet.

model. It is likely that the reduced bend-back of the field lines observed in the dusk sector is responsible for this systematic effect (through the first term on the right hand side of equation (7)).
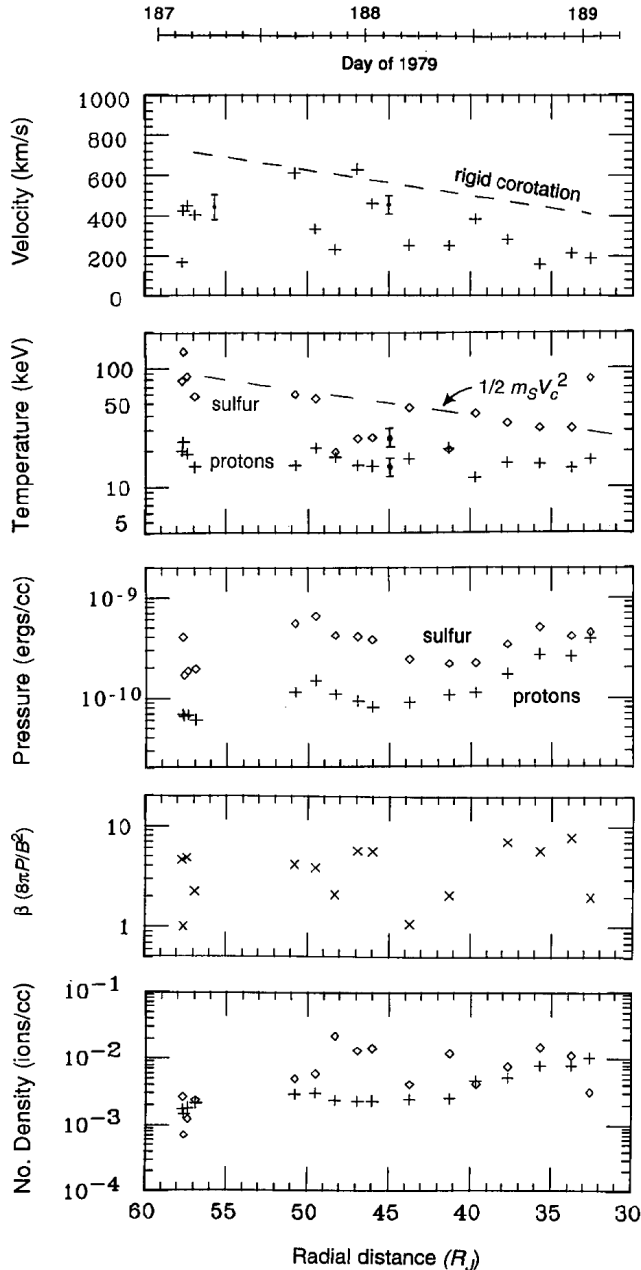
Figure 24.9. A moment analysis of the voyager 2 LECP particle flux data by Kane *et al.* (1995).

24.3.2 Thermal and Energetic Plasmas in the Middle Magnetosphere

The *Voyager* era observations of the plasma showed that the plasma is composed of two distinct components. A low energy component derived from Io's torus and called the warm or thermal plasma has a temperature of the order of 100 eV or less and diffuses outward (Siscoe and Summers, 1981). Another component called the energetic plasma has a temperature in excess of 20 keV and is believed to be heated and accelerated torus and solar wind plasma diffusing inward (Siscoe *et al.* 1981). Measurements of these plasma populations in the middle magnetosphere (McNutt *et al.* 1981, Krimigis et al., 1981) showed that the jovian plasma is indeed confined to a thin current sheet with an average half-

thickness of 2-3 R_J. Figure 24.6 shows the number density, temperature and flow velocity of the thermal plasma measured by *Voyager 1* in its inbound trajectory. The plasma number density is seen to fall from a peak value of 2000 particles/cm^3 in the cold Io torus to a value of less than 0.2 particles/cm^3 at a radial distance of ~ 35 R_J. The temperature of the thermal plasma is of the order of 100 eV in the middle magnetosphere. In addition, the plasma is seen to lag corotation beyond a radial distance of ~ 20 R_J.

Figure 24.7 shows differential fluxes of H$^+$, He$^+$, O$^+$ and S$^+$ ions for energies > 20 keV measured by the EPD experiment onboard *Galileo* at a radial distance of 25 R_J. Both protons and heavier iogenic plasma (O$^+$ and S$^+$) make important contributions to the differential fluxes. At energies greater than 1 MeV, the fluxes are dominated by the S$^+$ ions. Figure 24.8 shows the contribution of various species to the thermal particle pressure in the middle magnetosphere. Also plotted is the magnetic pressure difference (P$_{Blobe}$ − P$_{Bcsheet}$, solid circles) that balances the thermal pressure of the current sheet. It is evident that the energetic particles (E > 30 keV) carry almost all of the particle pressure that balances the magnetic pressure. Walker *et al.* (1978) using *Pioneer 10* observations and Lanzerotti *et al.* (1980) using *Voyager* 2 observations on specific current sheet crossings also reached similar conclusions.

Kane *et al.* (1995) deconvolved the full angular and spectral information from the *Voyager* 2 LECP instrument by using a nonlinear least squares technique that fits two-species convected κ distributions to the measured fluxes. Figure 24.9 show the ion density, plasma β, ion pressure, ion temperature and ion velocity obtained from their procedure. The derived parameters show that the temperature of the ions is close to 20 keV throughout this region and the velocity of the ions lags rigid corotation by as much as a factor of 2 in the middle magnetosphere.

The observations of the warm plasma from the *Galileo* plasma experiment (PLS) tend to confirm the findings of *Voyager* spacecraft. Frank *et al.* (2002) characterized the thermal plasmas and magnetic fields in the magnetotail using observations from the G7 orbit of the *Galileo* spacecraft around Jupiter (May 4 through June 22, 1997). This orbit traversed the magnetotail out to jovian radial distances of 100.2 R_J in the magnetotail. Perijove was positioned at 9.3 R_J. Three primary ion populations were detected with the plasma analyzer, cool hydrogen ions with temperatures of 10 eV, hot hydrogen ions with temperatures of about 10 keV, and a third population of heavy ions such as O^{++}, O$^+$ and S^{++}, and S^{+++} with temperatures in the range of 500 eV. Plasma flows near perijove were in the corotational direction (see Figure 24.10) but with speeds approximately 60% of those for rigid corotation out to radial distances of about 18 R_J. In the radial range of 18-26 R_J the bulk flow included significant radial components and the flow components in the corotational direction reached values expected for rigid corotation when the current sheet was crossed. The transient character of the plasma parameters suggests that strong ion plasma acceleration was occurring in this region. The temperatures of the heavy ions increased from 5×10^6 K at 9.3 R_J to about 10^8 K at 26 R_J. At distances < 20 R_J there was a strong dependence of ion temperatures on System III longitude. The scalar magnetic field outside of the current sheet in the radial distance range 9.3-20 R_J var-
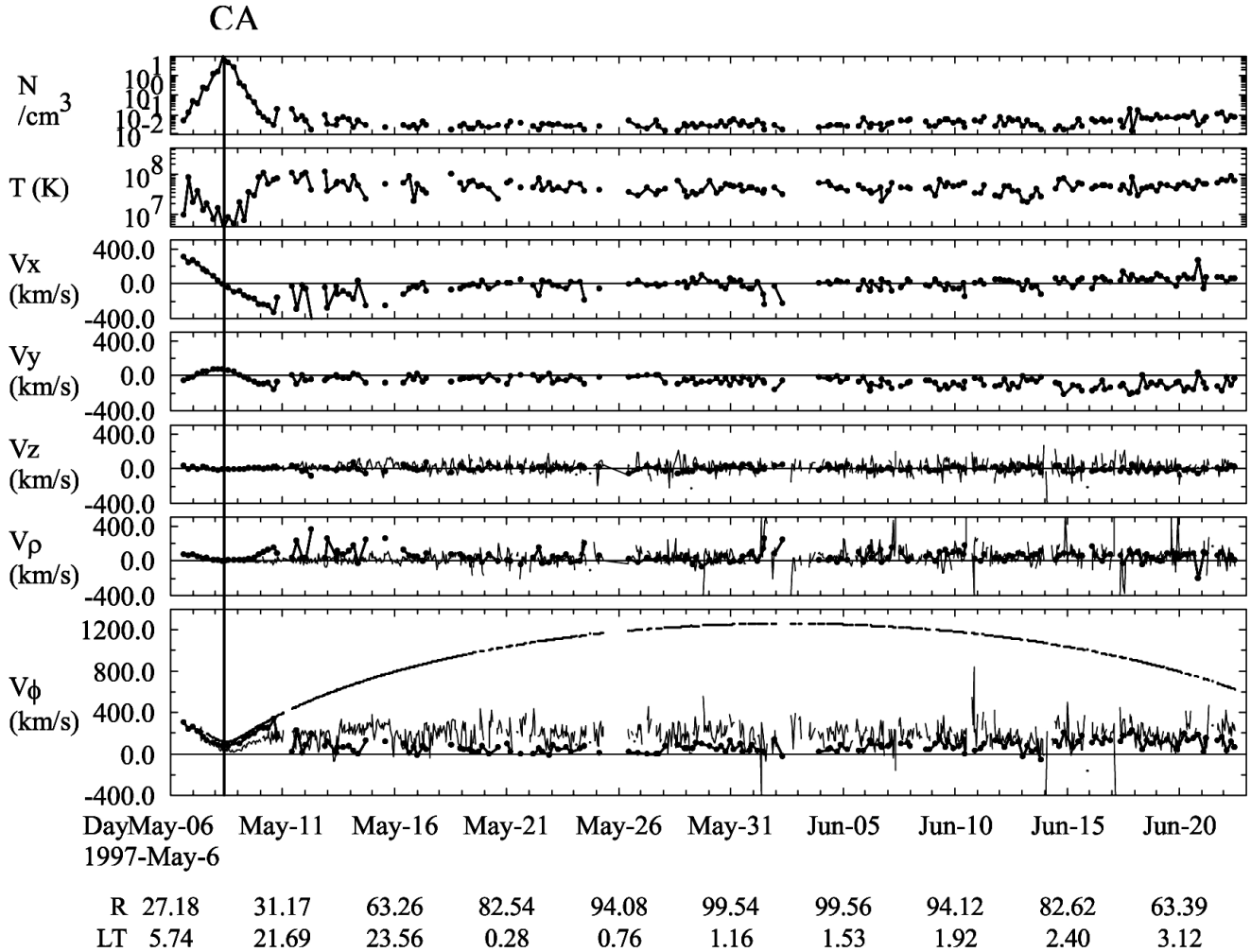
Figure 24.10. Survey plot for plasma parameters measured during the period May 5 to June 22, 1997: Plotted in black lines are: (panel 1) ion densities, (panel 2) ion temperatures, (panels 3-5) ion bulk flows in solar-ecliptic coordinates, (panel 6) ion bulk flow component in the radial direction and (panel 7) ion flow component in the corotational direction. These plasma moments are given for the crossings of the current sheet as determined with the simultaneous measurements of the magnetic fields. The jovicentric radial distance and local time of the spacecraft position are given along the abscissa. (Frank *et al.* 2002). Also shown, in gray, are the flow velocities (in km/s) in the north-south, radial, and azimuthal direction obtained from the first order anisotropies measured by the EPD instrument. The smooth curve in the bottom panel shows the corotation speed. CA = Clostest Approach of *Galileo* to Jupiter.

ied as R$^{-2.78}$ and similar to that for a dipole field, and at distances $> 50\ R_J$ as R$^{-1.19}$. The number densities and temperatures of these plasmas were 0.05-0.1 /cm^3 and 0.5-1 $\times$ 10^8 K, respectively. In the magnetotail the bulk flows of the thermal plasmas exhibited substantial components in the corotational and radially outwards directions, but the azimuthal speeds of 50-200 km/s were significantly less than those for rigid corotation. For this single orbit the average bulk flows were about 50 km/s in the pre-midnight sector and 200 km/s in the early morning sector at radial distances near 50 R_J. At apojove of 100 R_J an anti-sunward flow of about 200 km/s was found that is supportive of the magnetospheric "wind" reported for *Voyager* measurements of energetic charged particles. In addition to the ten-hour periodicity of the pairs of current sheet crossings at the position of the *Galileo* spacecraft, a variety of dynamical signatures were observed which could be related to the changes in di-

rection and pressures in the solar wind and to the transient acceleration of plasmas in the current sheet.

Also shown in red in the bottom three panels are the velocity components of the energetic plasma from the EPD instrument onboard *Galileo* during this interval. The velocity of the plasma is derived from the first order anisotropies in the fluxes measured by the EPD instrument (Krupp *et al.* 2001). It is seen that inside of 25 R$_J$, the two instruments are in rough agreement with each other. Beyond this distance, there is no one to one agreement between the flow velocities estimates provided by the EPD and the PLS instruments. However, both instruments show that in the middle and outer magnetosphere, the azimuthal velocity of the plasma is much lower than the corotational speed. It is not yet known whether the systematic differences seen in the radial component and the transient differences seen in bursty flows in all three components of flow are instrumental arti-
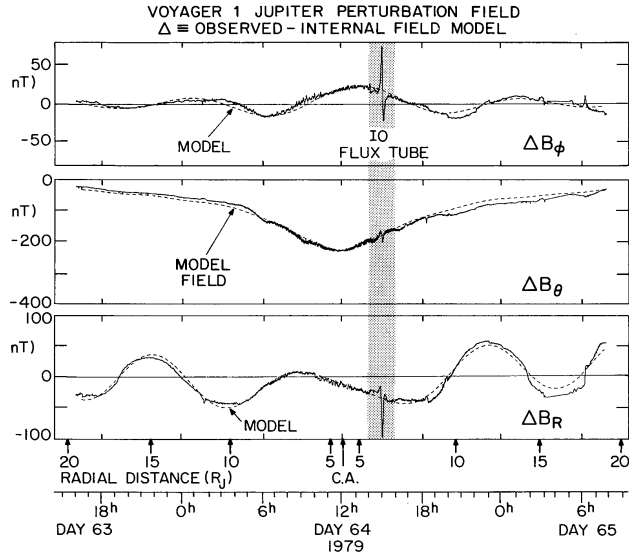
Figure 24.11. A comparison of the difference field with the Connerney *et al.* (1981) model. Figure reproduced from Connerney *et al.* (1981).

facts or are real and reflect the differences in the dynamics of warm and hot plasma populations.

24.3.3 Magnetic Field Models of the Current sheet

As discussed above, the structure of Jupiter's current sheet is very complex. From its origin in the centrifugal equator near Io's orbit, the current sheet moves closer to the dipole magnetic equator in the middle magnetosphere and ultimately becomes parallel to the solar wind in the magnetotail. The current sheet is also delayed in proportion to the radial distance of the observer. The field produced by the warped and delayed current sheet is equally complex and requires novel techniques to model it.

The first attempt to model the current sheet field was made by Connerney *et al.* (1981). They obtained explicit analytical solutions for the vector potential $\mathbf{A}$ that satisfies the relation $\mathbf{B} = \nabla \times \mathbf{A}$ in a semi-infinite azimuthally symmetric current sheet. They showed that an exact analytical solution can be obtained when the height-integrated current density in the current sheet is assumed to be equal to zero for $\rho < a$, and falls as I_0/ρ for $\rho > a$. The vector potential above (positive sign) and below (negative sign) the current sheet ($|z| > D$) is given by

$$A^{\pm}(\rho, z) = \mu_0 I_0 \int_0^{\infty} J_1(\rho\lambda) J_0(a\lambda) \sinh(D\lambda) e^{\mp z\lambda} \frac{d\lambda}{\lambda^2} \quad (10)$$

whereas inside the current sheet ($|z| < D$)

$$A(\rho, z) = \mu_0 I_0 \int_0^{\infty} J_1(\rho\lambda) J_0(a\lambda)(1 - e^{-D\lambda}\cosh(z\lambda)) \frac{d\lambda}{\lambda^2} \quad (11)$$

In order to obtain the field from an annular current sheet which has the azimuthal current flowing only in the region $a < \rho < b$, Connerney et al. superposed solutions

from two current sheets with inner edges at 6 and 30 R_J (and carrying currents in opposite directions). As the above solutions contain integrands, they are computationally very slow. Connerney *et al.* derived simple analytical functions which approximate these equations and allow fast computation of the field. Recently Edwards *et al.* (2001) have derived new analytical forms that provide more accurate approximations to the integral equations.

The agreement between Connerney *et al.*'s model and the observations from *Voyager* and *Pioneer* spacecraft inside of $6\,R_J < \rho < 30\,R_J$ is generally good (see Figure 24.11). However, beyond a radial distance of 30 R_J, the hinging and the lag of the current sheet become appreciable and the symmetric model becomes inapplicable.

Another approach which provides more satisfactory results at large radial distance uses Euler potentials to define the magnetic field. The idea is to represent the external magnetic field in terms of two scalar functions f and g (known as Euler potentials, Stern (1976)) through the relation:

$$\mathbf{B_e} = \nabla f(\rho, \varphi, Z) \times \nabla g(\rho, \varphi, Z) \quad (12)$$

Because

$$\mathbf{B_e} \cdot \nabla f = 0 \quad and \quad \mathbf{B_e} \cdot \nabla g = 0 \quad (13)$$

f and g are constant along any field line.

The starting point of such a model is the azimuthally symmetric infinite Harris current sheet which can be described by the Euler potentials:

$$f = -B_0 \rho D \ln\left[\cosh\left(z/D\right)\right], \quad g = \varphi \quad (14)$$

so that the magnetic field components are:

$$\begin{aligned} \mathbf{B} &= (B_\rho, B_\varphi, B_z) \quad (15) \\ &= \left[B_0 \tanh(z/D), \; 0, \; -B_0 \left(D/\rho\right) \ln[\cosh(z/D)]\right] \end{aligned}$$

Goertz *et al.* (1976) generalized the scalar potential f so that the modeled field would decrease with radial distance. In addition, they accounted for the bend-back of the field lines by distorting the scalar potential g as a function of radial distance.

$$\begin{aligned} f(\rho, Z) &= -\frac{b_0}{r^a}\left[\ln\left(\cosh\frac{z}{D}\right) + C\right] \quad (16) \\ g(\rho, \varphi) &= \varphi + 175(e^{\rho/500} - 1) \end{aligned}$$

The model was constructed to fit the *Pioneer 10* data and produces good agreement with the data beyond a radial distance of 20 R_J. However, the equations become singular near Jupiter and cannot be linked with the internal field models. Therefore, the model is unsuitable for studies which require tracing of field lines from the magnetosphere to the ionosphere. The Goertz et al. technique has since been improved by Khurana (1997) to remove the singularities in the model equations and couple it to the GSFC O_6 spherical harmonic model of the internal field. Khurana chose the following Euler potentials

$$\begin{aligned} f &= -C_1 \rho \left[\tanh(\frac{r_{01}}{r})\right]^{a_1} \ln\cosh\frac{(z - Z_{cs})}{D_1} \quad (17) \\ &\quad + \int \rho \left\{ C_2 \left[\tanh(\frac{\rho_{02}}{\rho})\right]^{a_2} \right. \end{aligned}$$
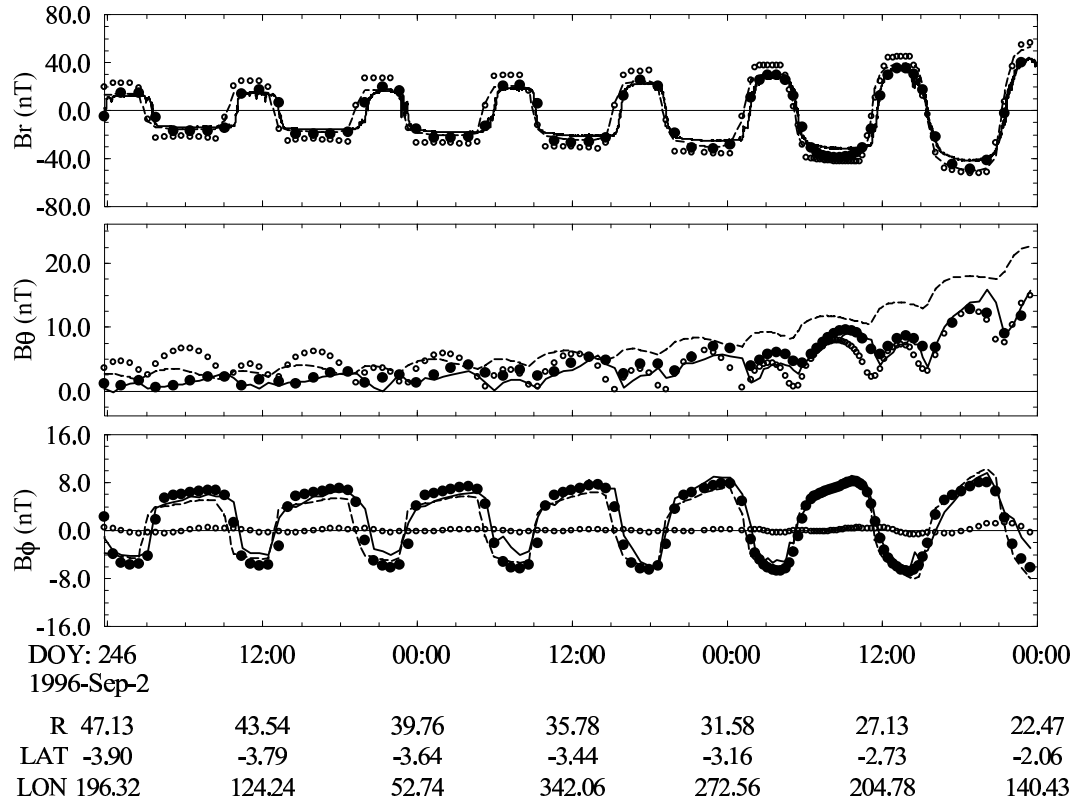
Figure 24.12. A comparison of the observed field from *Galileo's* G2 inbound orbit (solid lines) with the field calculated from the models of Connerney *et al.* (open circles), Goertz *et al.* (dashed lines) and Khurana (solid circles). Notice that the scales in the three panels are different.

$$+ C_3 \left[\tanh(\frac{\rho_{03}}{\rho})\right]^{a_3} + C_4 \Big\} d\rho$$

$$g = \varphi + p \left(1 + q \tanh^2 \frac{z - Z_{cs}}{D_2}\right) \rho \qquad (18)$$

The hinging and the delay of the current sheet is introduced through the term Z_{cs} in equation (17). Khurana (1997) chose the generalized hinged magnetodisc model (see equation (9) above) for this purpose. The models were constructed from data obtained in the dawn sector and consequently provide reliable estimates of the field in that sector (see Figure 24.12, where the models of Connerney *et al.* Goertz *et al.* and Khurana are compared with data from *Galileo's* G2 inbound orbit in the dawn sector).

24.3.4 The Structure of the Middle Magnetosphere

A long-standing debate in the magnetospheric community concerns the question whether solar wind and its embedded interplanetary magnetic field (IMF) play an appreciable role in driving convection in Jupiter's magnetosphere (Brice and Ioannidis, 1970; Kennel and Coroniti 1975). The potential energy available from corotation can be calculated from $\phi_{corotation} = \Omega_J \mathrm{B}_J \mathrm{R}_J^2$ which equals 376 MV for the known value of Jupiter's magnetic field. On the other hand, the solar wind induced electrical potential in Jupiter's polar cap is given by $\phi_{convection} = \varepsilon\ \mathrm{E}_0 \mathrm{Y}_{recon} = \varepsilon \mathrm{V}_{sw} \mathrm{B}_{IMF} \mathrm{Y}_{recon}$ where V_{sw} is the solar wind speed (≈ 400 km/s), B_{IMF} is

the IMF magnetic field (≈ 1 nT) and Y_{recon} is the length of the dayside magnetopause participating in reconnection (≈ 250 R$_J$). ε is a parameter known as "reconnection efficiency" and signifies the rate at which the IMF reconnection with the planetary magnetic field ($\approx 10\%$, in analogy with the rate observed in the Earth's magnetosphere). Thus $\phi_{convection} = 0.7$ MV. A simple comparison between the corotation potential and the solar wind induced polar cap potential would suggest that the latter is insignificant in determining the dynamics of Jupiter's magnetosphere. However, such a comparison ignores two important facts about the situation. The jovian corotation potential imparts acceleration to the plasma mainly in the azimuthal direction bringing it up to corotation and therefore does not directly participate in the radial transfer of magnetic flux. Secondly, the efficiency with which the corotation electric field available in the ionosphere is transferred to the magnetosphere is not known and may be very small if the ionospheric conductivity is not appreciable.

The influence of solar wind on the dynamics of Jupiter's magnetosphere can be gauged indirectly by studying the local time asymmetries present in the structure of magnetospheric field (see Figure 24.13). Before the arrival of *Galileo* at Jupiter, such a task was not feasible because only the noon and dawn sectors had been explored. However, with the availability of data from *Galileo*, the six spacecraft have now among them covered all local times of the low-latitude magnetosphere. In addition, *Ulysses* and *Pioneer 11* have provided information on the mid-latitude day and dusk regions
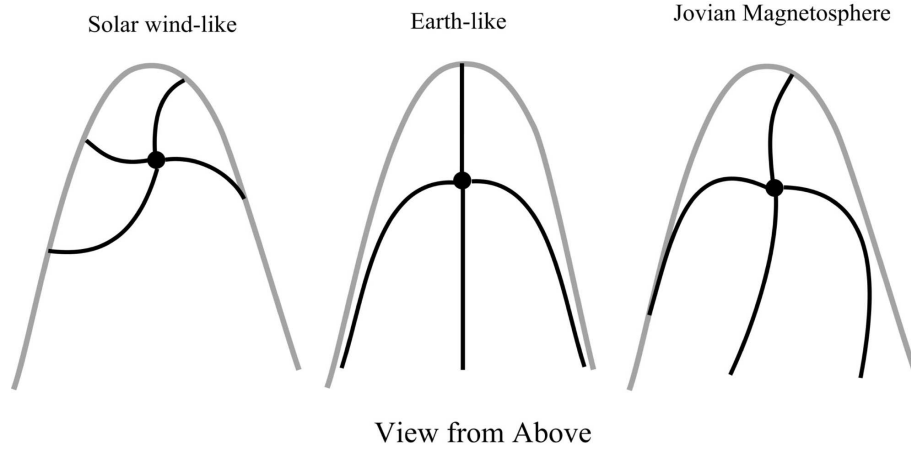
Solar wind-like   Earth-like   Jovian Magnetosphere

View from Above

Figure 24.13. Configuration of the magnetic field in a solar wind type outflow dominated system described by a Parker spiral (left), in the Earth's magnetosphere where the solar wind electric field drives strong convection (middle) and in Jupiter's magnetosphere as deduced by Khurana (2001).

of the magnetosphere. An analysis of the magnetic field from all six spacecraft was recently performed by Khurana (2001). Figure 24.14 reproduced below from this work shows the magnetic field perturbation vectors (observed field - internal field) plotted as unit vectors in an equatorial projection. Not surprisingly, the perturbation vectors show the influence of the solar wind in the boundary regions of the magnetosphere where the magnetic field is seen to become parallel to the magnetopause. But more significantly, a strong dawn-dusk asymmetry in the configuration of the field is also seen. On the dawnside, the field vectors make large angles to the radials and have a swept-back appearance consistent with plasma outflow and subcorotation of plasma. On the duskside, in the middle magnetosphere, the field vectors point essentially in the radial direction whereas in the outer magnetosphere they have a swept-forward appearance. Thus, it appears that the jovian magnetosphere has a magnetic field configuration that is intermediate to a Parker spiral and a magnetosphere driven by the solar wind (see Figure 24.13).

As electric currents are responsible for redistributing stresses in a plasma, a study of the current systems in a magnetosphere also provides insights into the agencies that control the magnetospheric dynamics. For example, it is well known in the Earth's magnetosphere (Iijima *et al.* 1990) that the azimuthal current strength is enhanced locally in the midnight sector. This enhanced current is called "the partial ring current" and is maintained by a global convection system driven by the solar wind. The enhanced azimuthal current on the nightside helps contain the larger plasma pressure observed in the nightside of the Earth's magnetosphere. The partial ring current is closed by a field-aligned current system called the "region 2" current system which draws out the current from the ionosphere in the dawn sector and returns it to the ionosphere in the dusk sector. Observations from *Galileo* now show that a similar current system (but with currents flowing in the opposite sense) exists in Jupiter's magnetosphere.

The magnetic field perturbation can be used to infer the electric current density in the equatorial plane of Jupiter under the assumption of a thin current sheet (Vasyliunas,
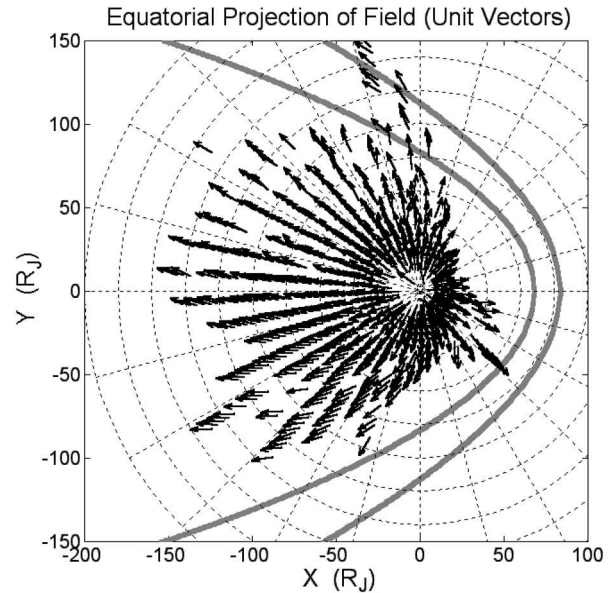

Figure 24.14. The magnetic field of the current sheet plotted as unit vectors on an equatorial grid (Reproduced from Khurana, 2001).

1983). For example, the azimuthal current can be obtained from (see Khurana, 2001)

$$J_\varphi = \frac{1}{\mu_0} \left(\frac{\partial \Delta B_\rho}{\partial z} - \frac{\partial \Delta Bz}{\partial \rho} \right) \qquad (19)$$

where ΔB_ρ and ΔB_z are the perturbation magnetic field (observed – internal) in the radial and axial directions, respectively. The integration of (19) over the thickness of the current sheet yields height integrated azimuthal current flowing through the current sheet per unit radial distance:

$$J'_\varphi = \int J_\varphi dz = \frac{1}{\mu_0} \left(2\Delta B_{\rho l} - 2w \frac{\partial \Delta B_z}{\partial \rho} \right) \qquad (20)$$

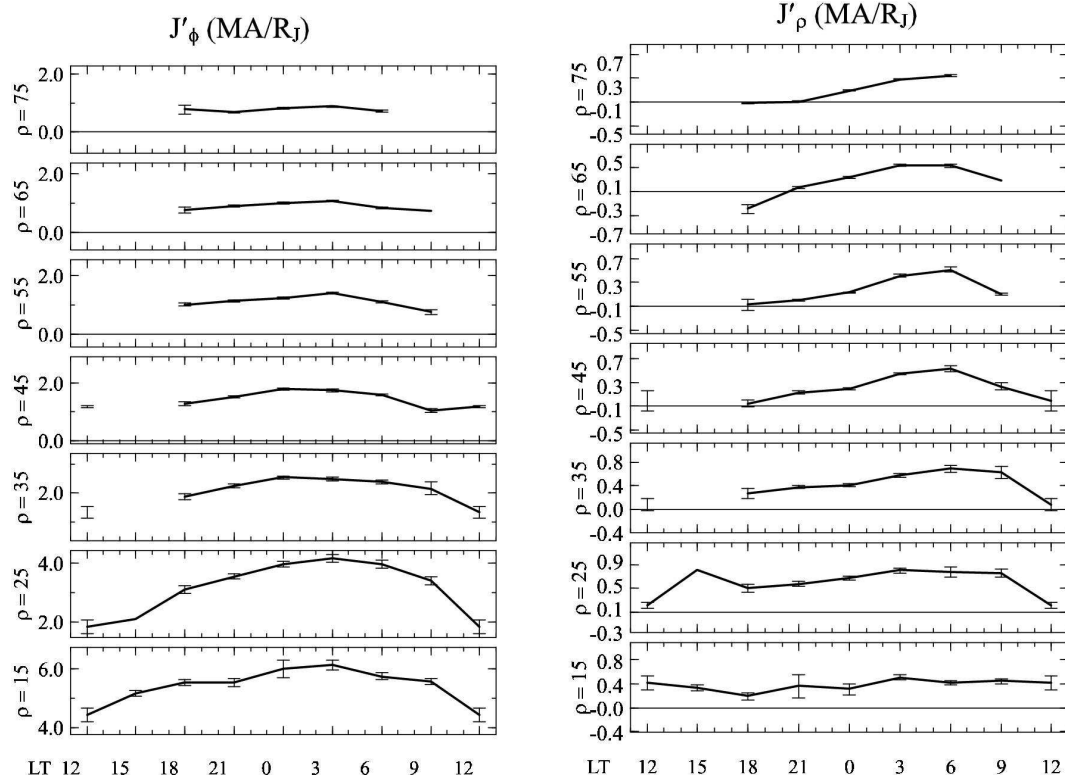where $\Delta B_{\rho l}$ is the radial component of the differenced mag-

J'_ϕ (MA/R$_J$)

J'_ρ (MA/R$_J$)

Figure 24.15. Binned height integrated azimuthal (left) and radial current density (right) in the equatorial plane of Jupiter's magnetosphere.
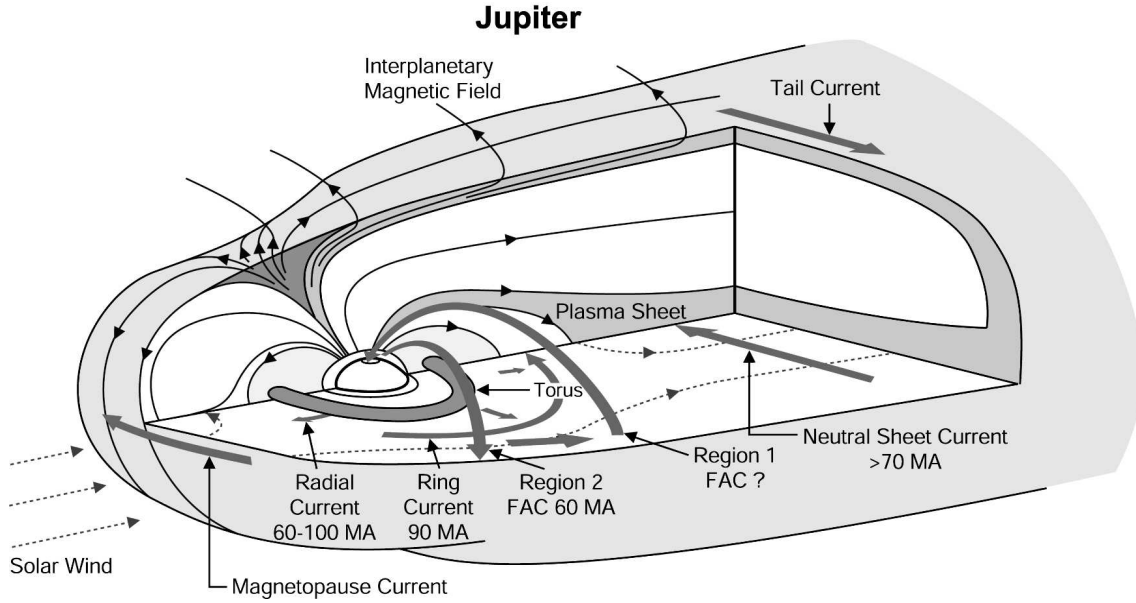

Figure 24.16. The strengths of the various current systems in Jupiter's magnetosphere. Figure adapted from Khurana (2001)

netic field just outside the current sheet (the lobe region) and w is the half-thickness of the current sheet.

Similarly, the radial component of the current density is obtained from

$$J_\rho = \frac{1}{\mu_0}\left(\frac{1}{\rho}\frac{\partial\,\Delta B_z}{\partial\,\varphi} - \frac{\partial\,\Delta B\varphi}{\partial\,z}\right) \qquad (21)$$

In Jupiter's magnetosphere, ΔB_z is not a strong function of local time. Therefore, the first term in equation (21) can be neglected. Integrating over z we obtain the height integrated radial current density:

$$J'_\rho = \int J_\rho\,dz = -\frac{2\Delta B_{\varphi l}}{\mu_0} \qquad (22)$$

where $\Delta B_{\varphi l}$ is the azimuthal component of the differenced magnetic field just outside the current sheet.

Figure 24.15 shows the azimuthal and radial current densities computed from the magnetic field data and binned into bin sizes of 10 R$_J$×3 hr bins. As expected, the azimuthal current density has a strong radial dependence falling from a peak value of $\sim$ 6 MA/R$_J$ in the innermost middle magnetospheric distances to a value of less than 1 MA/R$_J$ near 75 R$_J$. However, surprisingly the azimuthal current density has a strong variation with local time, being strongest near midnight and becoming small near noon. By using the concept of current continuity, Khurana (2001) has shown that a field-aligned current (FAC) system analogous to the Earth's region 2 FAC system (but opposite in direction) is required to feed and evacuate the jovian partial ring current. An inescapable conclusion of this discovery is that the solar wind influence reaches deep into the heart of Jupiter's magnetosphere.

The radial current density profiles show that in the radial distance range of 10-30 R$_J$, the current is directed outward and is quite uniform with local time. However, at distances > 30 R$_J$, the radial current density shows a marked local time dependence, maximizing near dawn and minimizing near dusk. Beyond a radial distance of $\sim$ 60 R$_J$ in the dusk region, the radial current changes sign, i.e. it is directed inward. The complex distribution of the radial current shows that a simple picture of a rotating-outflowing plasma in not valid for the whole of Jupiter's magnetosphere. It is likely that some of the complexity is caused by convection driven by the solar wind. Figure 24.16 adopted from Khurana (2001) provides a summary of the current systems and their strengths in Jupiter's magnetosphere.

24.3.5   Bend-Back of the Field and Plasma Outflow

As discussed above, the dominant source of plasma for Jupiter's magnetosphere is Io's torus located in the inner magnetosphere. The strong magnetic field of Jupiter provides an ideal trapping geometry for this plasma and only a small fraction of this plasma is able to precipitate on to Jupiter. The only escape route for this plasma is outflow through the magnetotail and magnetopause. The plasma outflow in the magnetosphere is driven by diffusion, interchange motion and reconnection with the IMF. Exactly how this plasma moves out is a topic of current debate and research and is further discussed below.

The effect of the plasma outflow on the field line geometry is significant. Viewed from above the north pole of Jupiter, the field lines in the dawn sector are seen to spiral out of their meridians by $\sim$ 40° within a radial distance of 100 R$_J$. The bend-back of the field lines can be understood as follows. As a parcel of plasma moves outward conserving its angular momentum, its angular velocity falls and the parcel starts to lag behind corotation. Because, the plasma is frozen to the magnetic field lines, it drags the field lines with it, which acquire a bent-back configuration. The bend back of the field line is equivalent to a radial current flowing away from the planet in the equatorial plane (see Figure 24.17). The current applies a $\mathbf{J} \times \mathbf{B}$ Lorentz force on the plasma to make it corotate. This interaction between the field and plasma results in a net outward transfer of angular
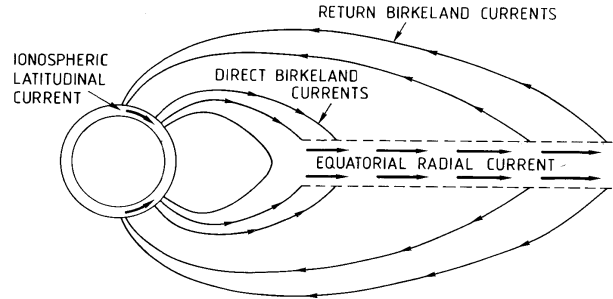

Figure 24.17. A schematic of the radially directed corotation enforcement current (CEC) that flows in the equatorial plane. The field-aligned Birkeland currents that close this current are also shown. Figure reproduced from Vasyliunas, 1983.
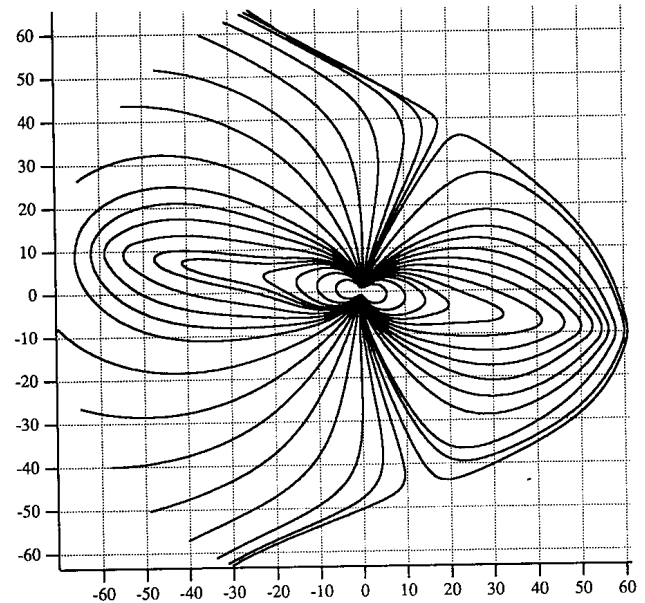

Figure 24.18. Magnetic field lines from the Engle (1992) magnetic field model of jovian magnetosphere.

momentum from the ionosphere of Jupiter to the outflowing plasma. The corotation of plasma cannot continue for indefinitely large distances and must break down where the ionosphere is not able to impart sufficient angular momentum to the magnetosphere. By assuming a constant outflow rate and a finite conductivity of the ionosphere Hill, (1979) showed that the equatorial distance L_0 where this breakdown is expected to occur is given by

$$L_0(R_J) = 64(\Sigma/0.1 \text{ mho})^{-1/4}(M/10^{28} \text{ amu}/s)^{-1/4} \qquad (23)$$

The observations indeed show (Khurana and Kivelson, 1993) that the torque applied by the magnetic field on plasma keeps on increasing up to a distance of $\sim$ 50-60 R$_J$ and then levels off. On the other hand, the torque required to keep the plasma in corotation increases as ρ^2. The plasma subcorotation results from the difference between these two torques. New observations of the radial currents from previous missions and *Galileo* tend to confirm this picture (Bunce and Cowley, 2001, Khurana, 2001). It has also become clear

that the origin of Jupiter's main auroral oval lies in these corotation enforcement currents (CEC) that link Jupiter's auroral region to the magnetosphere (Hill, 2001, Cowley and Bunce 2001, Khurana, 2001). Barbosa *et al.* (1981) had indirectly inferred the presence of these field-aligned currents and associated field-aligned potentials from a study of impulsive electrostatic emissions that were localized to the jovian middle magnetosphere (10 $R_J < R < 30$ R_J). This subject is further explored in chapter 28.

As discussed above, a clear dawn to dusk local time asymmetry is also present in the distribution of the radial current. Because, there is no understandable reason for the ionospheric conductivity to have a dawn to dusk asymmetry, the implication of radial current asymmetry is that the plasma outflow rate may be non-uniform in local time.

If the plasma losses within the magnetosphere were small, the mass outflow rate $S = \rho \int \sigma_m U_\rho d\phi$ (where σ_m is the height integrated mass density) would be expected to remain constant with radial distance. Russell *et al.* (2000) have exploited this fact to determine the effective outflow velocity of plasma in the jovian magnetosphere. They assumed that the mass outflow rate is uniform with local time and System III longitude and obtained the height integrated mass density estimates from the tangential momentum equation. The expected values of the plasma velocity are near tens of meters/s in the inner torus to several hundred kilometers/s in the outer magnetosphere.

24.4 THE OUTER MAGNETOSPHERE

24.4.1 The Chapman-Ferraro Currents

Another source of external field in a magnetosphere is the Chapman-Ferraro magnetopause current system. The field from this "distant" source can also be described in terms of a potential as $\mathbf{B}_e = -\nabla\Phi_e$ whose solution in terms of spherical harmonics is given by:

$$\Phi_e = R\sum_{l=1}^{\infty}\left(\frac{r}{R}\right)^l \sum_{m=0}^{l} P_l^m(\cos\theta) \quad (24)$$
$$[G_l^m \cos(m\lambda) + H_l^m \sin(m\lambda)]$$

where R is the planet's radius, r, θ and λ are the radial distance, colatitude and the longitude of the observer, P_l^m are the associated Legendre polynomial functions and G_l^m, H_l^m are the Schmidt coefficients of order l and degree m determined from the observations.

On the dayside of the planet, where the magnetopause has a spherical shape, the spherical harmonics provide an excellent description of the magnetopause field. However, at large distances along the magnetotail, the spherical harmonics rapidly diverge and provide unsatisfactory result (see for example, Figure 24.18 reproduced from Engle (1992)). It is therefore, advantageous to express the contribution of the magnetopause currents in spheroidal (Sotirelis *et al.* 1994), cylindrical or Cartesian harmonics (Tsyganenko, 1995). For example, Tsyganenko (1995) expressed the external field potential from currents in the Earth's magnetopause as:

$$\Phi_e = \sum_{i=1}^{N}\left[A_i J_1\left(\frac{\rho}{b_i}\right)\exp\left(\frac{X}{b_i}\right)\sin\phi \quad (25)\right.$$
$$\left. + C_i J_0\left(\frac{\rho}{d_i}\right)\exp\left(\frac{X}{d_i}\right)\right]$$

where J_0 and J_1 are Bessel functions, X is the planetocentric distance along the sun-planet direction, ρ is the distance from the sun-planet line and A_i, C_i, a_i, b_i, c_i and d_i are the coefficients and scale factors to be determined from the observations.

The only attempts to include the contribution of the magnetopause currents in a global magnetic field have been made by Engle and colleagues (Engle and Beard 1980, Engle 1991, 1992). Their global models incorporate a thin current sheet co-located with the dipole equator, an internal potential field and a magnetic field arising from the shielding currents flowing along the magnetopause. Their last model (Engle 1992) also allows for an arbitrary tilt of the dipole. This was made possible by the use of interpolations of spherical harmonics obtained for several discrete dipole tilts. Unfortunately, because of the choice of the harmonic series to express the field of the magnetopause (spherical rather than Cartesian or cylindrical harmonics which are better suited for currents arising from a paraboloidal surface, see equation (25) above), the model is not able to reproduce the field of the stretched magnetotail reliably on the nightside (see Figure 24.18). In addition, the model lacks a realistic current sheet geometry (warping and delay) and the sweepback of the field lines.

24.4.2 Magnetotail

A magnetotail forms downstream of a magnetized planet as a direct consequence of momentum transfer between the magnetosphere and the solar wind. Two different phenomena - viscous interaction and direct solar wind momentum entry – contribute to the structure and dynamics of the magnetotail. If the magnetosphere is closed, the momentum transfer occurs mainly from the viscous interactions between the solar wind and the magnetospheric plasmas at the boundaries of the magnetosphere. The magnetotail of a closed magnetosphere is relatively short (a few D_{mp} where D_{mp} is the length scale of the magnetosphere in the subsolar direction) so that the magnetosphere has a teardrop shape (Song *et al.* 1999). However, if the magnetosphere is open, direct entry of solar wind density and momentum flux can occur. The magnetotail then contains two lobe regions above and below the central current sheet which house open magnetotail flux connected on one end to the planet and at the other end to the IMF. The magnetotail of an open magnetosphere tends to be very long (as much as several hundred D_{mp}). For example, the Earth's magnetotail has been encountered at a distance of over a thousand R_E downstream of the Earth (Behannon, 1970). In an open magnetotail, the enhanced magnetic pressure of the lobes compresses the central current sheet causing it to thin. Jupiter's magnetotail also appears to belong to this class. Scarf et al. (1981), Kurth *et al.* (1982) and Lepping *et al.* (1983) have reported entries of *Voyager* 2 into the magnetotail of Jupiter when the space-

craft was just upstream of Saturn at a distance of ~ 7000 R$_J$ from Jupiter.

The first detailed studies of Jupiter's magnetotail became possible when the two *Voyagers* explored the dawn region of the magnetotail to a radial distance of ~ 100 R$_J$ in 1979. Behannon *et al.* (1981) showed that Jupiter's magnetotail contains a thin current sheet (half-thickness ~ 2 R$_J$) surrounded by lobes mostly devoid of plasma. The field magnitude in the lobes was seen to decrease as a power law with an exponent of -1.4 which is considerably faster than that observed in the Earth's lobes (B$_L$ $\propto$ X$^{-0.5}$ at distances out to 130 R$_E$, Slavin et al. (1985)). New observations from *Galileo*, which explored the magnetotail to a distance of 150 R$_J$, tend to confirm this picture. Kivelson and Khurana (2002a) have shown that the average lobe field over all local times falls as B$_L \propto \rho^{-1.37}$. The faster fall off at Jupiter is accounted by the fact that the lobe field at Jupiter has been characterized at distances of 2 to 3 D_{mp} whereas the Earth's studies apply to distances of 10-13 D_{mp}.

The Kivelson and Khurana (2002a) study also shows that the flux tubes are less stretched on the dusk side than they are on the dawn side. The difference is caused mainly by the local time variations of the field component normal to the current sheet (B$_\theta$). In the same radial distance range of ~ 40–100 R$_J$, the normal component is found to be almost twice as strong on the dusk side as it is on the dawn side. This is illustrated in Figure 24.19 where we show magnetic field observations from *Galileo* in the radial range of 35–55 R$_J$ from an inbound trajectory on the dawn side (thick lines) and an outbound trajectory on the dusk side (thin lines). In addition to a weaker normal component (B_θ) on the dawn side, one finds that the spacecraft spent considerable time in both the north and the south lobes (where the field plateaus at positive and negative constant values). When the spacecraft emerges from one lobe and approaches the other, the change in the sign of the radial component is rapid, indicating that the current sheet is very thin (half thickness < 1.5 R$_J$). On the other hand in the dusk side, the spacecraft fails to enter either of the lobes indicating that h must be greater than $\sim 45 \tan (9.6°) = 7.6$ R$_J$. The difference in the current sheet thickness can be explained by postulating that the distribution of the open flux is asymmetric across the magnetotail (see Figure 24.20). This would imply that the magnetotail is mostly open on the dawnside but closed up to very high latitudes on the duskside. This postulate is consistent with the observations of bi-directional streaming of electrons and ions observed by *Ulysses* during its mid-latitude *dusk* pass (Staines *et al.* 1996; Krupp *et al.* 1997). Bi-directional streaming of plasma is caused by mirroring of particles on closed field lines. On the other hand, energetic particle observations from the dawn side from *Galileo* and other spacecraft are consistent with the lobe regions being essentially open. For example, the electron fluxes (60 keV – 31 MeV) observed in the dawn sector by the University of Iowa experiment onboard *Pioneer 10* showed that when the spacecraft was in the lobe regions, the particle counts dropped to the background values seen in the magnetosheath (Van Allen *et al.* 1974).

Differences in the distribution of open flux across the tail can be explained by invoking convection in a single (dawnside) cell in Jupiter's magnetosphere. This is certainly possible considering the fact that corotation would augment
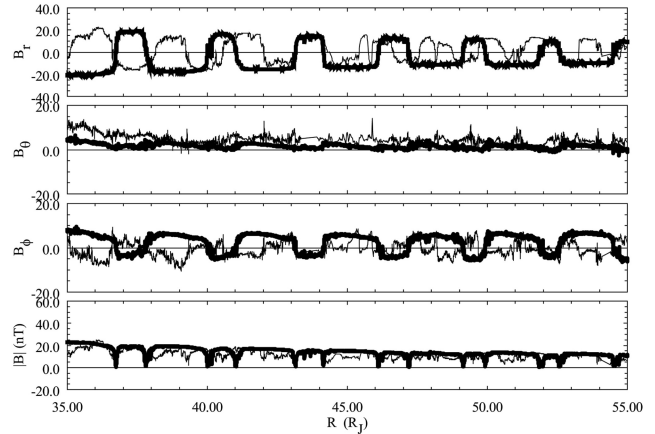

Figure 24.19. Observed magnetic field from *Galileo* during a dawn pass (G2, thick lines) and a dusk pass (C23, thin lines).

the return flow from a reconnection region in the magnetotail on the dawn side but would oppose it on the dusk side. The corotation therefore tends to switch off the solar wind driven convection on the duskside. This would reduce the amount of open flux in the dusk sector.

Figure 24.19 shows another difference between the dawn and the dusk sectors of Jupiter's magnetosphere. The bend-back of the field lines - apparent from an anti-correlation between the radial and azimuthal components of the magnetic field - is stronger on the dawn side compared to its value on the dusk side. Kivelson *et al.* (2002) have shown that at a radial distance of ~ 100 R$_J$ in the dusk sector, the field lines are twisted in the direction of corotation lag near the plasma sheet, but at higher latitudes they are twisted forward in the direction leading corotation. A similar situation was observed by *Ulysses*, which exited the jovian magnetosphere at mid latitudes in the dusk sector (Dougherty *et al.* 1993). Kivelson *et al.* further show that the dominant cause of the bend forward are the field aligned currents that are flowing into the ionosphere. This field-aligned current must be at least partially fed by the CEC flowing radially outward. It is also likely that a part of the current system consists of Region 1 type FAC (Iijima and Potemra, 1976) whose origin is a viscous convection cell driven by the solar wind at the flanks of the magnetosphere (Sonnerup, 1980).

24.5   PLASMA DIFFUSION AND CONVECTION: HOW PLASMA MOVES OUTWARD

The rapid rotation of Jupiter together with the large size of its magnetosphere in comparison to the planet suggested early on that the plasma within the magnetosphere predominantly corotates with the planet, an inference first made by Brice and Ioannidis (1970) on the basis of a simple quantitative model (generalized slightly by Vasyliunas (1975)). Pure corotation, however, provides no path for removal of plasma from the magnetosphere, and losses by precipitation into the atmosphere of Jupiter are easily shown to be small (essentially because of, again, the small size of the planet compared to the magnetosphere). It was therefore suggested by Ioannidis and Brice (1971) that the resulting accumula-
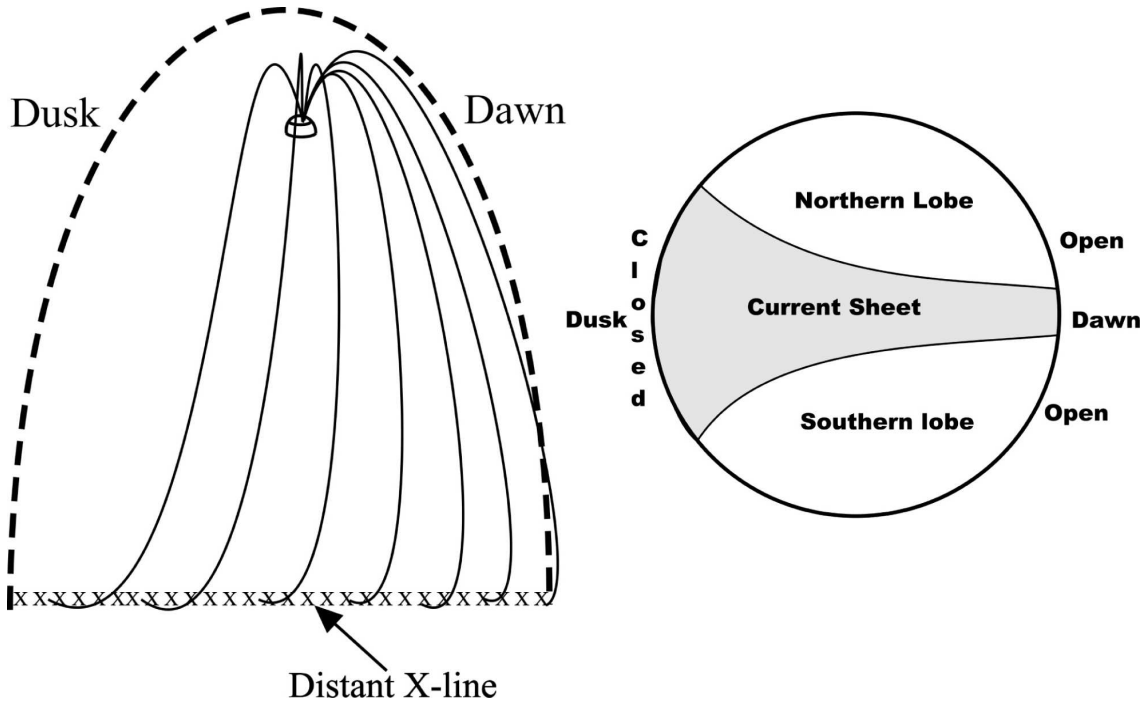
Figure 24.20. The structure of the magnetotail as viewed from above (left) and in a YZ cross-section near X = 50 R$_J$.

tion of plasma would lead to its outward transport by an interchange instability driven by centrifugal stresses, while Michel and Sturrock (1974) proposed that beyond some distance the magnetic field would be too weak to contain the corotating plasma, which would break the field lines open and flow out radially as a planetary wind, but only on the night side where there is no confining pressure by the solar wind (Hill *et al.* 1974). Recent discovery of sharply bounded, radially moving flux tubes which display enhanced levels of magnetic flux and broadband low frequency electromagnetic waves have provided the first hints of interchange driven transport (Bolton *et al.* 1997; Kivelson *et al.* 1997; Thorne *et al.* 1997).

This basic pattern of plasma flow - corotation within the magnetosphere, combined with some type of radial transport, changing to radial outflow within the magnetotail - was thus theoretically expected already prior to the discovery of the Io torus. The transition from corotation to radial outflow necessarily involves reconnection of magnetic field lines; the simplest model of the associated topological changes was sketched by Vasyliunas [1983, Fig. 11.19]. The discovery of the Io torus, by establishing that the primary source of plasma lies in the vicinity of the Io orbit and hence deep within the inner magnetosphere, has impacted our understanding of plasma flow in several ways.

It has focused attention on the transport process, from the Io source across the region of closed magnetic field lines to the outer magnetosphere. Incompletely understood, this process is generally assumed to proceed by some form of interchange motions of magnetic flux tubes (discussed in more detail in Chapter 25).

As discussed above, to maintain corotation during this transport process, conservation of angular momentum requires a continuous stress to be exerted by currents closing through the ionosphere, and Hill (1979) has shown that the ionospheric conductivity is too small for this beyond a characteristic equatorial distance R$_H$ (Hill corotation radius) of the field line. The same considerations of angular momentum imply a small localized reduction of corotational flow in the source region where newly ionized plasma is accelerated to (near) corotation [Pontius and Hill, 1982], an effect evident in the Io torus (see Chapter 23) but of little global significance.

The greatly reduced speed of corotation at distances beyond R$_H$ may require previous arguments for the predominance of corotation and for the breaking open of field lines to be reconsidered.

24.5.1   Observations

It has not yet been possible to determine the complete average configuration of plasma bulk flow in the jovian magnetosphere from observations. Extensive measurements of plasma flow parameters are, however, available and can generally be interpreted in the context of the expected patterns described above, albeit with some modifications or extensions. Among the main results are the following:

In the inner and middle magnetosphere, the flow is predominantly in the corotational direction, at nearly the full corotation speed close in, becoming slower than corotation with increasing distance, and leveling off at a roughly constant speed of ~ 200 km s^{-1} in the magnetotail (McNutt *et al.* 1981; Kane *et al.* 1995, Frank and Paterson, 2001, Krupp et al., 2001).

The qualitative behavior agrees with the model of Hill (1979), but the limiting value in the magnetotail is much higher than expected (Pontius, 1997), and there is a local-time variation not predicted by the axially symmetric model:
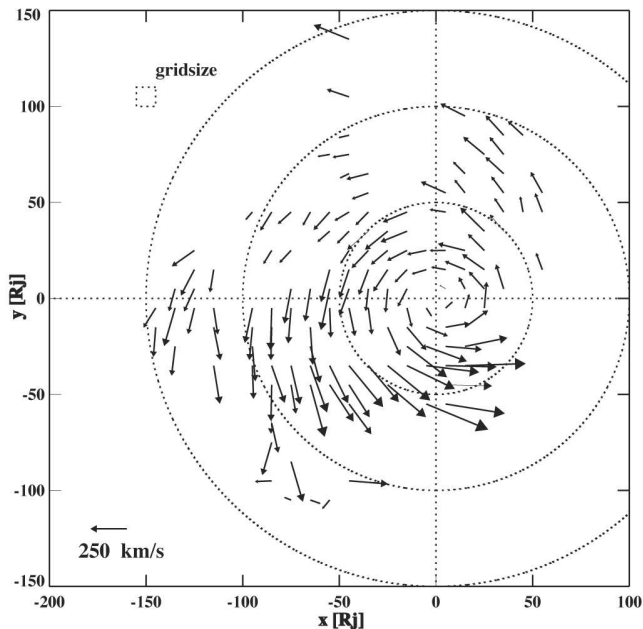
Figure 24.21. Average flow pattern in the magnetosphere of Jupiter.

the azimuthal flow is slower in the pre-midnight sector and approaches closer to corotation near dawn (Krupp *et al.* 2001, Frank and Paterson, 2001). Figure 24.21 shows the average flow pattern in Jupiter's magnetosphere.

More or less persistent radially outward or antisunward flows have been observed in the distant magnetotail (Krimigis *et al.* 1981, Frank and Paterson 2001) and may be related to planetary-wind processes. Significant radial flows are also observed at closer distances in the magnetotail, but they are generally highly variable and are most likely related to dynamical events: they may be directed either outward or inward and are often accompanied by variations of the magnetic field and the plasma of a form that is suggestive of magnetic reconnection processes (Russell et al., 1998) These events are discussed in more detail in Chapter 25.

Within the Io plasma torus, fluctuations of plasma flow about the mean corotation have been observed, accompanied by fluctuations of density, magnetic field, and energetic particles. The properties of the observed fluctuations are plausibly consistent with those expected for interchange motions postulated to drive the plasma transport process, but whether they in fact account for the transport has not yet been conclusively determined. For further discussion, see Chapter 25.

24.6 PLASMA ACCELERATION AND HEATING IN JUPITER'S MAGNETOSPHERE

24.6.1 Ionization and Charge Exchange

The initial energy of plasma particles in the magnetosphere is fixed by the ionization process, in which a new charged particle (either by itself, in the case of electron impact or photoionization, or accompanied by removal of a pre-existing particle, in the case of charge exchange) with the

speed of the original neutral particle is placed within the streaming ambient plasma. Since the neutral particle was moving at something like the Keplerian speed while the plasma is streaming at the corotation speed or some fraction of it, the newly injected charged particle is accelerated by the electric field of the plasma flow and acquires an energy corresponding to the velocity difference between the neutral gas and the plasma. The process is discussed in detail, including important collision and radiation effects, in Chapters 20 and 23. The final result is a plasma with bulk flow nearly equal to corotation, ion temperature lower than corotational energy by about an order of magnitude, and electron temperature lower by almost another order of magnitude.

24.6.2 Adiabatic Pocesses

Radial transport of plasma particles involves changes of energy that can be described in two equivalent ways: the result of either the conservation of the first and the second adiabatic invariants (the third invariant must be violated if a net radial displacement is to occur) or of adiabatic compression/expansion in the changing volume of the magnetic flux tube. The energy increases for inward and decreases for outward displacements; with a fixed distance of the source region, the mean energy decreases with increasing equatorial radial distance of the flux tube. Long known for the Earth's radiation belts, this process was proposed for Jupiter (Brice and McDonough, 1973), with assumption of a source region near the magnetosphere boundary, in order to explain the electron radiation belt needed to account for the observed synchrotron emissions (see e.g. Coroniti, 1975, and references therein; up-to-date discussion in Chapter 27).

The general increase of energy with decreasing radial distance expected from this process is in agreement with most observations of plasma and charged particles in the inner and middle magnetosphere. One exception is the cold plasma torus, which, however, can be understood at least in part on the basis of atomic-physics processes important on the long time scales presumed relevant (see Chapter 23). Another possible exception is the ion temperature profile in the Io torus, which has been reported as increasing with increasing radial distance from *Voyager* (Belcher, 1983) and also from *Galileo* (Frank and Paterson, 2001b) observations. Ground-based observations of the torus (Herbert and Hall, 1998, Thomas *et al.* 2001; see also Chapter 23), on the other hand, have been interpreted as showing the expected decreasing temperature with increasing distance within the center of the torus, with possible higher temperatures at higher latitudes as predicted by non-Maxwellian models, and it has been suggested (Herbert and Hall, 1998) that the *Voyager* results may be affected by the spacecraft's higher latitude at larger distances. The question of how the torus ion temperature varies with radius and whether therefore an additional, non-adiabatic heating process is needed is not yet fully settled.

A particular variant of adiabatic acceleration, proposed to account for the observation of very energetic (MeV-range) particles in the outer magnetosphere, is the so-called recirculation model suggested by Nishida (1976) and in a different form by Goertz (1978). Both models exploit the different behavior of particles mirroring at low latitudes, near the

equator, and at high latitudes, near the planet, together with assumed pitch angle scattering to transfer particles from one group to the other. Nishida has particles adiabatically compressed in the usual way by inward transport of entire flux tubes, followed by enhanced scattering across field lines at low altitudes (the result of wave turbulence at frequencies higher than the bounce frequency) and hence with little energy change, which brings the energized particles back to the outer flux tubes, where they undergo pitch-angle scattering and are again adiabatically compressed by inward transport. Goertz invokes the fact that corotation paths in the magnetosphere distorted by the solar wind takes particles from high (day side) to low (night side) equatorial field strengths, with consequent large changes of energy for particles mirroring near the equator but small changes for those at high latitudes; switching between equatorial and high-latitude paths by pitch-angle scattering then leads to diffusion in energy. The applicability of these models remains uncertain. In terms of location and energy range, they might be viewed as alternative explanations for what may also be attributed to magnetic reconnection.

24.6.3   Reconnection and Magnetotail Processes

Particle acceleration and heating in current sheets and near magnetic singular lines associated with magnetic reconnection has been extensively studied in the Earth's magnetosphere. There is now considerable evidence that analogous events occur at Jupiter, as discussed in Chapter 25.

24.6.4   Low-Altitude and Auroral Processes

Aurora on Jupiter is discussed in Chapter 26. It has been interpreted largely in terms of terrestrial analogs, with the assumption that low-altitude acceleration and heating processes related ultimately to intense Birkeland (magnetic-field-aligned) electric currents between the magnetosphere and the ionosphere are responsible. Evidence for such processes is provided by observations of intense beams of electrons, with energies from the 100 eV to the 100 keV range, at various locations in the magnetosphere (Bhattacharya *et al.* 2001; Frank and Patterson, 2002). These beams are aligned with the magnetic field, within an angular width too small to be resolved by the available instruments (i.e. less than a few degrees). Almost the only plausible explanation for such narrow alignment is that these particles have been accelerated at sufficiently low altitudes to produce the alignment by conservation of the first adiabatic invariant. The observed locations and intensities of the electron beams are consistent with the assumed auroral association.

24.7   LOCAL TIME ASYMMETRIES: INFLUENCE OF SOLAR WIND

The solar wind influences the structure and dynamics of a magnetosphere in two different ways. First, through the differences of external pressure, the solar wind creates a noon-midnight asymmetry in the magnetospheric field strength (accompanied by the corresponding requisite asymmetries of Chapman-Ferraro and magnetotail current systems). This is a magnetostatic effect that has no direct influence on plasma

motions (other than setting boundary conditions). Second, reconnection of the interplanetary magnetic field with the planetary field allows mass and momentum to be exchanged between the solar wind and the magnetosphere. This produces a global convection system which may further redistribute field and plasma in the planet's magnetosphere. For example, in the Earth's magnetosphere plasma is convected inward from the magnetotail and adiabatically compressed in the dipole field. The resulting pressure distribution, however, is not azimuthally symmetric (despite the symmetry of the dipole field) but tends to peak near midnight due to a complicated interaction between convection and magnetic drifts. The corresponding asymmetry in the currents whose force balances the pressure gradients implies a partial ring current centered on the nightside (Iijima *et al.* 1990), which ultimately closes into the Earth's ionosphere through region-2 sense field-aligned currents, part of those that couple the Earth's magnetosphere with its ionosphere. Thus it is clear that, in determining the nature of field and plasma asymmetries, the role of solar wind on a planetary magnetosphere is one of the primary factors.

As discussed above in the section on the outer magnetosphere, the magnetotail of Jupiter is remarkably asymmetric across its dawn and dusk flanks (see the discussion following Figures 24.19 and 24.20). Differences between the dawn and dusk sectors are typically produced by rotational flow interacting with the noon-midnight asymmetry. Solar-wind driven convection tends rather to produce midnight different from the flanks. Some of the observed asymmetries may, however, be interpreted as the result of convection confined to the dawn side only. In addition, a partial ring current system (see discussion following Figure 24.16) with an associated field-aligned current system is also present in Jupiter's magnetosphere.

The Jovian partial ring current system appears to be similar in many respects to the partial ring current system in the Earth's magnetosphere. The latter is generally explained as the result (through indirect and rather subtle processes) of a global convection system driven by the solar wind. This similarity may be taken as an indication that solar-wind- driven convection plays a significant role at Jupiter, analogous to its role at Earth, exerting a major control on the structure and dynamics of the Jovian magnetosphere even while the bulk of latter's mass and momentum derive from internal sources. Alternatively, it may be taken as an indication that partial ring currents occur generally in magnetotails and are not restricted to the particular processes occurring at Earth. An unambiguous conclusion in this regard must await further analysis of data from *Galileo*.

24.8   OUTSTANDING ISSUES

Even though early investigations of the data from the *Galileo* mission have provided many new insights into the structure and the workings of Jupiter's magnetosphere, several questions still remain unanswered. There is no doubt that further detailed analysis of data from *Galileo* and new data from future spacecraft missions will help answer many of these questions. The following are some of the major outstanding issues in the area of structure and convection of Jupiter's magnetosphere at this time.

• How does the inner magnetosphere convection driven by interchange instability combine with the convection driven by the solar wind electric field in the outer magnetosphere? Is the torus plasma ultimately lost mainly through the magnetotail?

• How are the low energy torus plasmas in Jupiter's magnetosphere heated to energies of tens of keV to MeV observed in the middle magnetosphere?

• What are the various sources of local time asymmetries observed in the field, plasma and electric current environments?

• How are the corotation enforcement currents closed? New observations have clearly linked the auroral region with the field-aligned currents drawn out of the ionosphere. These field-aligned currents feed the corotation enforcement currents in the current sheet. Ultimately, this current has to return to the ionosphere. However, it is not yet clear how and where (along high latitude field lines or along magnetopause etc.) this current returns to the ionosphere.

• Why is there no direct correlation between the strength of the corotation enforcement currents and the strength of the auroral brightness? The auroral images show that the integrated emission flux is much larger on the dusk side compared to its value on the dawn side. However, as discussed above, the radially outward corotation enforcement currents peak on the dawn side.

• What is the cushion region? How is it formed? Is it always present or is it a transient phenomenon?

REFERENCES

Acuna, M. H. and N. F. Ness, The main magnetic field of Jupiter, *J. Geophys. Res.* **81**, 2917–2922, 1976.

Bagenal, F., Empirical model of the Io plasma torus: *Voyager* measurements, *J. Geophys. Res.* **99**, 11,043–11,062, 1994.

Bagenal, F., Ionization source near Io from *Galileo* wake data, *Geophys. Res. Lett.* **24**, 2111, 1997.

Bagenal, F. and J. D. Sullivan, Direct plasma measurements in the Io torus and inner magnetosphere of Jupiter, *J. Geophys. Res.* **86**, 8447–8466, 1981.

Bagenal, F., R. L. McNutt, J. W. Belcher, H. S. Bridge, and J. D. Sullivan, Revised ion temperatures for *Voyager* plasma measurements in the Io plasma torus, *J. Geophys. Res.* **90**, 1755–1757, 1985.

Barbosa, D. D., F. L. Scarf, W. S. Kurth, and D. A. Gurnett, Broadband electrostatic noise and field-aligned currents in Jupiter's middle magnetosphere, *J. Geophys. Res.* **86**, 8357–8369, 1981.

Behannon, K. W., Magnetic fields in the Earth's tail, in *Particles and Field in the Magnetosphere*, p. 157, 1970.

Behannon, K. W., L. F. Burlaga, and N. F. Ness, The jovian magnetotail and its current sheet, *J. Geophys. Res.* **86**, 8385–8401, 1981.

Belcher, J. W., The low-energy plasma in the jovian magnetosphere, in *Physics of the Jovian Magnetosphere, A.J. Dessler (ed), Cambridge University Press*, pp. 68–105, 1983.

Bhattacharya, B., R. M. Thorne, and D. J. Williams, On the energy source for diffuse jovian auroral emissivity, *Geophys. Res. Lett.* **28**, 2751, 2001.

Bolton, S. J., R. M. Thorne, D. A. Gurnett, W. S. Kurth, and D. J. Williams, Enhanced whistler-mode emissions: Signatures of interchange motion in the Io torus, *Geophys. Res. Lett.* **24**, 2123, 1997.

Bolton, S. J., S. M. Levin, S. L. Gulkis, M. J. Klein, R. J. Sault, B. Bhattacharya, R. M. Thorne, G. A. Dulk, and Y. Leblanc, Divine-Garrett model and jovian synchrotron emission, *Geophys. Res. Lett.* **28**, 907, 2001.

Brice, N. M. and G. A. Ioannidis, The magnetospheres of Jupiter and Earth, *Icarus* **13**, 173, 1970.

Brice, N. M. and T. R. McDonough, Jupiter's radiation belts, *Icarus* **18**, 206–219, 1973.

Broadfoot, A. L., B. R. Sandel, D. E. Shemansky, J. C. McConnell, G. R. Smith, J. B. Holberg, S. K. Atreya, T. M. Donahue, D. F. Strobel, and J. L. Bertaux, Overview of the *Voyager* ultraviolet spectrometry results through Jupiter encounter, *J. Geophys. Res.* **86**, 8259–8284, 1981.

Bunce, E. J. and S. W. H. Cowley, Local time asymmetry of the equatorial current sheet in Jupiter's magnetosphere, *Planet. Space Sci.* **49**, 261–274, 2001.

Connerney, J. E. P. and M. H. Acuna, Jovimagnetic secular variation, *Nature* **297**, 313–315, 1982.

Connerney, J. E. P., M. H. Acuna, and N. F. Ness, Modeling the jovian current sheet and inner magnetosphere, *J. Geophys. Res.* **86**, 8370–8384, 1981.

Connerney, J. E. P., M. H. Acuna, and N. F. Ness, *Voyager* 1 assessment of Jupiter's planetary magnetic field, *J. Geophys. Res.* **87**, 3623–3627, 1982.

Connerney, J. E. P., M. H. Acuña, N. F. Ness, and T. Satoh, New models of Jupiter's magnetic field constrained by the Io flux tube footprint, *J. Geophys. Res.* **103**, 11,929–11,940, 1998.

Cooper, J. F., R. E. Johnson, B. H. Mauk, H. B. Garrett, and N. Gehrels, Energetic ion and electron irradiation of the icy Galilean satellites, *Icarus* **149**, 133–159, 2001.

Coroniti, F. V., Dénouement of jovian radiation belt theory, in *The Magnetospheres of the Earth and Jupiter*, p. 391, 1975.

Cowley, S. W. H. and E. J. Bunce, Origin of the main auroral oval in Jupiter's coupled magnetosphere-ionosphere system, *Planet. Space Sci.* **49**, 1067–1088, 2001.

Davis, L. and E. J. Smith, The jovian magnetosphere and magnetopause, in *Magnetospheric Particles and Fields*, pp. 301–310, 1976.

Divine, N. and H. B. Garrett, Charged particle distributions in Jupiter's magnetosphere, *J. Geophys. Res.* **88**, 6889–6903, 1983.

Dougherty, M. K., D. J. Southwood, A. Balogh, and E. J. Smith, Field-aligned currents in the jovian magnetosphere during the *Ulysses* flyby, *Planet. Space Sci.* **41**, 291–300, 1993.

Dougherty, M. K., A. Balogh, D. J. Southwood, and E. J. Smith, *Ulysses* assessment of the jovian planetary field, *J. Geophys. Res.* **101**, 24,929–24,942, 1996.

Edwards, T. M., E. J. Bunce, and S. W. H. Cowley, A note on the vector potential of Connerney et al.'s model of the equatorial current sheet in Jupiter's magnetosphere, *Planet. Space Sci.* **49**, 1115–1123, 2001.

Engle, I. M., Idealized *Voyager* jovian magnetosphere shape and field, *J. Geophys. Res.* **96**, 7793–7802, 1991.

Engle, I. M., Diurnal variation in jovian subsolar magnetopause position, *J. Geophys. Res.* **97**, 17,169, 1992.

Engle, I. M. and D. B. Beard, Idealized jovian magnetosphere shape and field, *J. Geophys. Res.* **85**, 579–592, 1980.

Frank, L. A. and W. R. Paterson, Passage through Io's ionospheric plasmas by the *Galileo* spacecraft, *J. Geophys. Res.* **106**, 26,209–26,224, 2001a.

Frank, L. A. and W. R. Paterson, Survey of thermal ions in the

Io plasma torus with the *Galileo* spacecraft, *J. Geophys. Res.* **106**, 6131–6150, 2001b.

Frank, L. A., W. R. Paterson, and K. K. Khurana, Observations of plasmas in the jovian magnetotail with the *Galileo* spacecraft, *J. Geophys. Res.* pp. 1–1, 2002.

Goertz, C. K., The current sheet in Jupiter's magnetosphere, *J. Geophys. Res.* **81**, 3368–3372, 1976.

Goertz, C. K., Energization of charged particles in Jupiter's outer magnetosphere, *J. Geophys. Res.* **83**, 3145–3150, 1978.

Goertz, C. K., The orientation and motion of the predawn current sheet and Jupiter's magnetotail, *J. Geophys. Res.* **86**, 8429–8434, 1981.

Herbert, F. and D. T. Hall, Disentangling electron temperature and density in the Io plasma torus, *J. Geophys. Res.* **103**, 19,915–19,926, 1998.

Hide, R. and D. Stannard, Jupiter's magnetism - Observations and theory, in *Jupiter, T. Gehrels (ed), University of Arizona Press*, pp. 767–787, 1976.

Higgins, C. A., T. D. Carr, F. Reyes, W. B. Greenman, and G. R. Lebo, A redefinition of Jupiter's rotation period, *J. Geophys. Res.* **102**, 22,033–22,041, 1997.

Hill, T. W., Inertial limit on corotation, *J. Geophys. Res.* **84**, 6554–6558, 1979.

Hill, T. W., The jovian auroral oval, *J. Geophys. Res.* **106**, 8101–8108, 2001.

Hill, T. W., A. J. Dessler, and C. K. Goertz, Magnetospheric models, in *Physics of the Jovian Magnetosphere, A.J. Dessler (ed), Cambridge University Press*, pp. 353–394, 1983.

Iijima, T. and T. A. Potemra, The amplitude distribution of field-aligned currents at northern high latitudes observed by Triad, *J. Geophys. Res.* **81**, 2165–2174, 1976.

Iijima, T., T. A. Potemra, and L. J. Zanetti, Large-scale characteristics of magnetospheric equatorial currents, *J. Geophys. Res.* **95**, 991–999, 1990.

Ioannidis, G. and N. Brice, Plasma densities in the jovian magnetosphere: Plasma slingshot or Maxwell demon?, *Icarus* **14**, 360, 1971.

Joy, S. P., M. G. Kivelson, R. J. Walker, K. K. Khurana, C. T. Russell, and T. Ogino, Probabilistic models of the jovian magnetopause and bow shock locations pp. 17–1, 2002.

Kane, M., B. H. Mauk, E. P. Keath, and S. M. Krimigis, Hot ions in Jupiter's magnetodisc: A model for *Voyager* 2 low-energy charged particle measurements, *J. Geophys. Res.* **100**, 19,473–19,486, 1995.

Kennel, C. F. and F. V. Coroniti, Is Jupiter's magnetosphere like a pulsar's or Earth's?, in *The Magnetospheres of the Earth and Jupiter, ASSL*, p. 451, 1975.

Khurana, K. K., A generalized hinged-magnetodisc model of Jupiter's nightside current sheet, *J. Geophys. Res.* **97**, 6269–6276, 1992.

Khurana, K. K., Euler potential models of Jupiter's magnetospheric field, *J. Geophys. Res.* **102**, 11,295–11,306, 1997.

Khurana, K. K., Influence of solar wind on Jupiter's magnetosphere deduced from currents in the equatorial plane, *J. Geophys. Res.* **106**, 25,999–26,016, 2001.

Khurana, K. K. and M. G. Kivelson, Inference of the angular velocity of plasma in the jovian magnetosphere from the sweep-back of magnetic field, *J. Geophys. Res.* **98**, 67–79, 1993.

Kivelson, M. G. and K. K. Khurana, Properties of the magnetic field in the jovian magnetotail pp. 23–1, 2002.

Kivelson, M. G., P. J. Coleman, L. Froidevaux, and R. L. Rosenberg, A time dependent model of the jovian current sheet, *J. Geophys. Res.* **83**, 4823–4829, 1978.

Kivelson, M. G., K. K. Khurana, C. T. Russell, and R. J. Walker, Intermittent short-duration magnetic field anomalies in the Io torus: Evidence for plasma interchange?, *Geophys. Res. Lett.* **24**, 2127, 1997.

Kivelson, M. G., K. K. Khurana, and R. J. Walker, Sheared mag-

netic field structure in Jupiter's dusk magnetosphere: Implications for return currents pp. 17–1, 2002.

Krimigis, S. M., J. F. Carbary, E. P. Keath, C. O. Bostrom, W. I. Axford, G. Gloeckler, L. J. Lanzerotti, and T. P. Armstrong, Characteristics of hot plasma in the jovian magnetosphere - Results from the *Voyager* spacecraft, *J. Geophys. Res.* **86**, 8227–8257, 1981.

Krupp, N., E. Keppler, R. Seidel, J. Woch, A. Korth, A. F. Cheng, S. E. Hawkins, L. J. Lanzerotti, C. G. Maclennan, and M. K. Dougherty, Field-particle streaming in the duskside high latitude jovian magnetosphere, *Adv. Space Res.* **20**, 225, 1997.

Krupp, N., A. Lagg, S. Livi, B. Wilken, J. Woch, E. C. Roelof, and D. J. Williams, Global flows of energetic ions in Jupiter's equatorial plane: First-order approximation, *J. Geophys. Res.* **106**, 26,017–26,032, 2001.

Kurth, W. S., D. A. Gurnett, J. D. Sullivan, H. S. Bridge, F. L. Scarf, and E. C. Sittler, Observations of Jupiter's distant magnetotail and wake, *J. Geophys. Res.* **87**, 10,373–10,383, 1982.

Lanzerotti, L. J., C. G. Maclennan, S. M. Krimigis, T. P. Armstrong, K. W. Behannon, and N. F. Ness, Statics of the nightside jovian plasma sheet, *Geophys. Res. Lett.* **7**, 817–820, 1980.

Lepping, R. P., M. D. Desch, E. C. Sittler, K. W. Behannon, L. W. Klein, J. D. Sullivan, and W. S. Kurth, Structure and other properties of Jupiter's distant magnetotail, *J. Geophys. Res.* **88**, 8801–8815, 1983.

McNutt, R. L., J. W. Belcher, and H. S. Bridge, Positive ion observations in the middle magnetosphere of Jupiter, *J. Geophys. Res.* **86**, 8319–8342, 1981.

Michel, F. C. and P. A. Sturrock, Centrifugal instability of the jovian magnetosphere and its interaction with the solar wind, *Planet. Space Sci.* **22**, 1501–1510, 1974.

Mihalov, J. D., H. M. Fischer, E. Pehlke, and L. J. Lanzerotti, Energetic trapped electron measurements from the *Galileo* Jupiter probe, *Geophys. Res. Lett.* **27**, 2445, 2000.

Nishida, A., Outward diffusion of energetic particles from the jovian radiation belt, *J. Geophys. Res.* **81**, 1771–1773, 1976.

Pontius, D. H., Radial mass transport and rotational dynamics, *J. Geophys. Res.* **102**, 7137–7150, 1997.

Pontius, D. H. and T. W. Hill, Departure from corotation of the Io plasma torus - Local plasma production, *Geophys. Res. Lett.* **9**, 1321–1324, 1982.

Randall, B. A., An improved magnetic field model for Jupiter's inner magnetosphere using a microsignature of Amalthea, *J. Geophys. Res.* **103**, 17,535, 1998.

Russell, C. T., K. K. Khurana, D. E. Huddleston, and M. G. Kivelson, Localized reconnection in the near jovian magnetotail, *Science* **280**, 1061, 1998.

Russell, C. T., M. G. Kivelson, K. K. Khurana, and D. E. Huddleston, Circulation and dynamics in the jovian magnetosphere, *Adv. Space Res.* **26**, 1671–1676, 2000.

Russell, C. T., Z. J. Yu, and M. G. Kivelson, The rotation period of Jupiter, *Geophys. Res. Lett.* **28**, 1911, 2001.

Scarf, F. L., W. S. Kurth, D. A. Gurnett, H. S. Bridge, and J. D. Sullivan, Jupiter tail phenomena upstream from Saturn, *Nature* **292**, 585, 1981.

Schardt, A. W. and C. K. Goertz, High-energy particles, in *Physics of the Jovian Magnetosphere, A.J. Dessler (ed), Cambridge University Press*, pp. 157–196, 1983.

Schardt, A. W., F. B. McDonald, and J. H. Trainor, Energetic particles in the predawn magnetotail of Jupiter, *J. Geophys. Res.* **86**, 8413–8428, 1981.

Scudder, J. D., E. C. Sittler, and H. S. Bridge, A survey of the plasma electron environment of Jupiter - A view from *Voyager*, *J. Geophys. Res.* **86**, 8157–8179, 1981.

Siscoe, G. L. and D. Summers, Centrifugally driven diffusion of iogenic plasma, *J. Geophys. Res.* **86**, 8471–8479, 1981.

Siscoe, G. L., A. Eviatar, R. M. Thorne, J. D. Richardson,

F. Bagenal, and J. D. Sullivan, Ring current impoundment of the Io plasma torus, *J. Geophys. Res.* **86**, 8480–8484, 1981.

Slavin, J. A., E. J. Smith, D. G. Sibeck, D. N. Baker, and R. D. Zwickl, An ISEE 3 study of average and substorm conditions in the distant magnetotail, *J. Geophys. Res.* **90**, 10,875, 1985.

Sloanaker, R. M., Apparent temperature of Jupiter at a wave length of 10 cm., *AJ* **64**, 346–346, 1959.

Song, P., D. L. DeZeeuw, T. I. Gombosi, C. P. T. Groth, and K. G. Powell, A numerical study of solar wind-magnetosphere interaction for northward interplanetary magnetic field, *J. Geophys. Res.* **104**, 28,361, 1999.

Sonnerup, B. U. O., Theory of the low-latitude boundary layer, *J. Geophys. Res.* **85**, 2017–2026, 1980.

Sotirelis, T., N. A. Tsyganenko, and D. P. Stern, Method for confining the magnetic field of the cross-tail current inside the magnetopause, *J. Geophys. Res.* **99**, 19,393, 1994.

Staines, K., A. Balogh, S. W. H. Cowley, T. M. Edwards, R. J. Forsyth, R. J. Hynds, and N. F. Laxton, An overview of the anisotropy telescope observations of MeV ions during the *Ulysses* Jupiter encounter, *Planet. Space Sci.* **44**, 341–369, 1996.

Stern, D. P., Representation of magnetic fields in space, *Rev. Geophys. Space Phys.* **14**, 199–214, 1976.

Thomas, N., G. Lichtenberg, and M. Scotto, High-resolution spectroscopy of the Io plasma torus during the *Galileo* mission, *J. Geophys. Res.* **106**, 26,277–26,292, 2001.

Thorne, R. M., T. P. Armstrong, S. Stone, D. J. Williams, R. W. McEntire, S. J. Bolton, D. A. Gurnett, and M. G. Kivelson, *Galileo* evidence for rapid interchange transport in the Io torus, *Geophys. Res. Lett.* **24**, 2131, 1997.

Tsyganenko, N. A., Modeling the Earth's magnetospheric magnetic field confined within a realistic magnetopause, *J. Geophys. Res.* **100**, 5599–5612, 1995.

Vasyliunas, V. M., Concepts of magnetospheric convection, in *The magnetospheres of the Earth and Jupiter*, p. 179, 1975.

Vasyliunas, V. M., Plasma distribution and flow, in *Physics of the Jovian Magnetosphere, A.J. Dessler (ed), Cambridge University Press*, pp. 395–453, 1983.

Vogt, R. E., W. R. Cook, A. C. Cummings, T. L. Garrard, N. Gehrels, E. C. Stone, J. H. Trainor, A. W. Schardt, T. Conlon, N. Lal, and F. B. McDonald, *Voyager* 1 - Energetic ions and electrons in the jovian magnetosphere, *Science* **204**, 1003–1007, 1979.

Walker, R. J., M. Kivelson, and A. W. Schardt, High beta plasma in the dynamic jovian current sheet, *Geophys. Res. Lett.* **5**, 799–802, 1978.